



UNITED NATIONS EDUCATIONAL, SCIENTIFIC AND CULTURAL ORGANIZATION
INTERNATIONAL ATOMIC ENERGY AGENCY
INTERNATIONAL CENTRE FOR THEORETICAL PHYSICS
I.C.T.P., P.O. BOX 586, 34100 TRIESTE, ITALY, CABLE: CENTRATOM TRIESTE



SMR/930 - 27

**"Workshop on El Niño, Southern Oscillation and Monsoon"
15 - 26 July 1996**

"Role of Seasonal Cycle in the ENSO/Monsoon System"

T. YASUNARI
University of Tsukuba
Ibaraki
Japan

Please note: These are preliminary notes intended for internal distribution only.

Role of Seasonal Cycle in the ENSO/monsoon System

Tetsuzo Yasunari

Institute of Geoscience, University of Tsukuba,
Ibaraki, 305, Japan

1. Tropospheric Biennial Oscillation (TBO)
in the ENSO/monsoon system
2. Seasonality of TBO and the "monsoon year"
3. Possible mechanisms of TBO
 - 3.1 Atmosphere-ocean interaction in the warm pool region
 - 3.2 Land-atmosphere-ocean interaction
through winter and summer monsoon in Asia
4. What determines ENSO or non-ENSO events ?
Possible role of NAO and the chaos in the extra-tropics

BO signals in the Monsoon/ENSO system

- o Rainfall (convection)
- o SST
- o wind

* One anomalous year tends to be followed by the preceded year with opposite anomaly

* Seasonality

- from boreal summer to the following spring
- "monsoon year"

インドモンスーン降水量 と エル・ニニョ発現

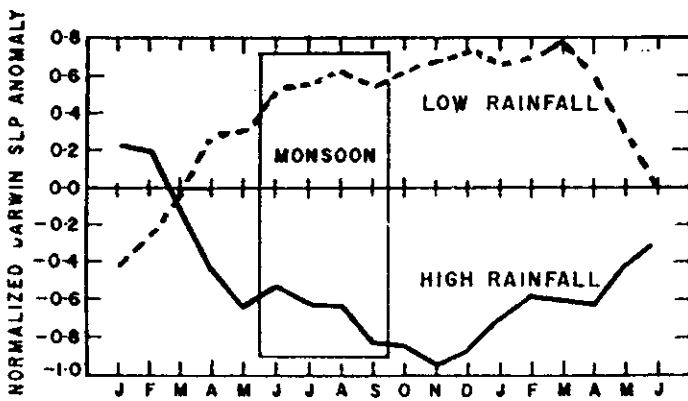
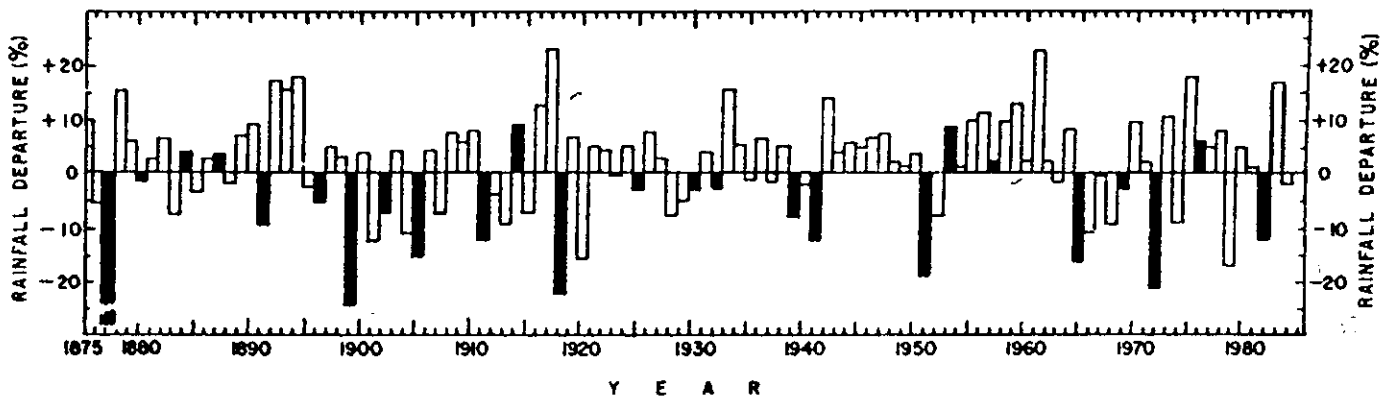
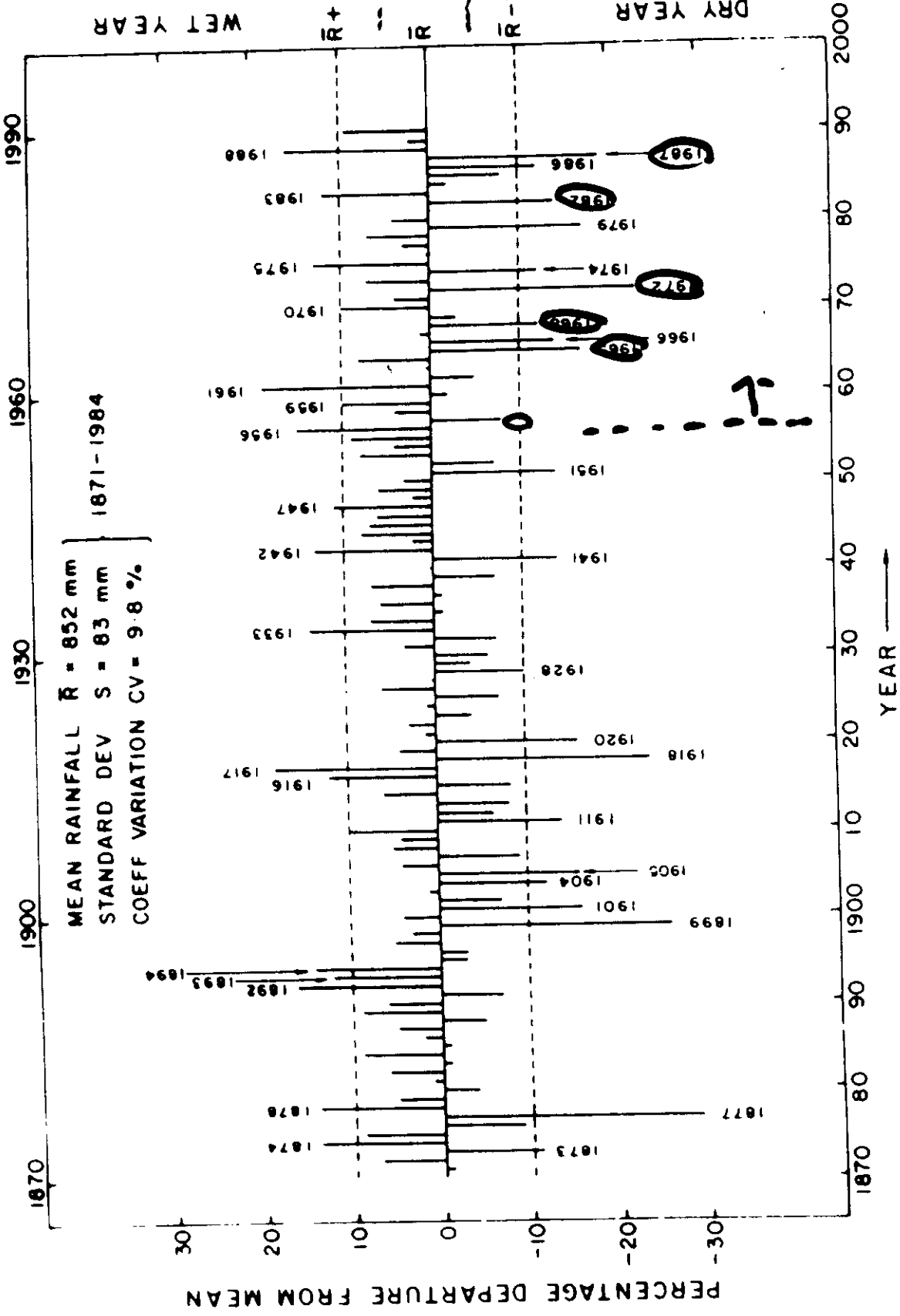
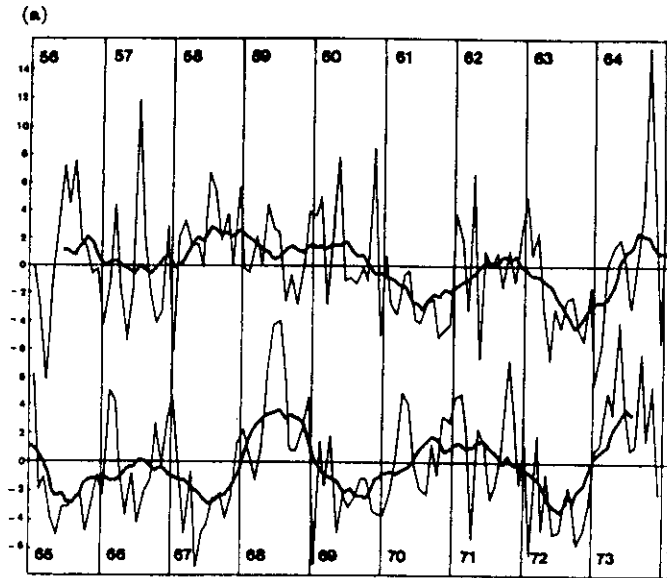


Figure 42: *Top*: Monsoon rainfall over India expressed in percentage departure, with *El Niño* events indicated by black shaded pillars (from Mooley and Shukla, 1985). *Left*: Composite of normalized Darwin pressure anomaly (3-month running mean) for heavy monsoon rainfall years (solid), and deficient monsoon rainfall years (dashed) (from Shukla and Paolino, 1983).

ALL-INDIA SUMMER MONSOON RAINFALL

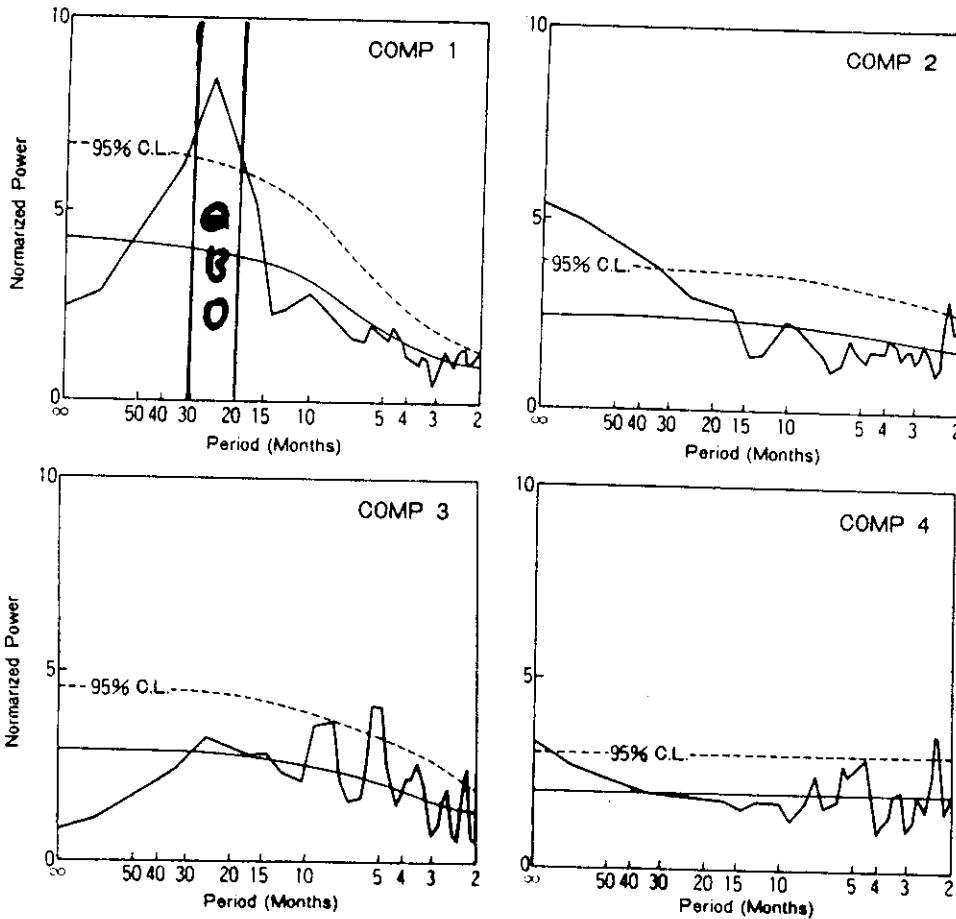


YEAR-TO-YEAR PERCENTAGE DEPARTURE FROM MEAN OF ALL-INDIA SUMMER MONSOON RAINFALL FROM THE YEAR 1871 ONWARDS EXCESS / DEFICIENT YEARS ARE MARKED AGAINST BARS



PCA-1
 INDONESIAN
 MONTHLY RAINFALL
 (54 stations)

T. YASUNARI: Temporal and Spatial Variations of Monthly Rainfall in Java, Indonesia



QBO
 in the PCA-1
 Indonesian
 Rainfall.

Fig. 8 Power spectra of the time coefficients for the first to the fourth component. Power spectrum is normalized by dividing them by the variance of each component. The red noise or white noise level (thin solid line), and the limit of the 95% confidence level (dashed line) are also shown in each case. (Yasunari, 1981)

QBO in Rainfall

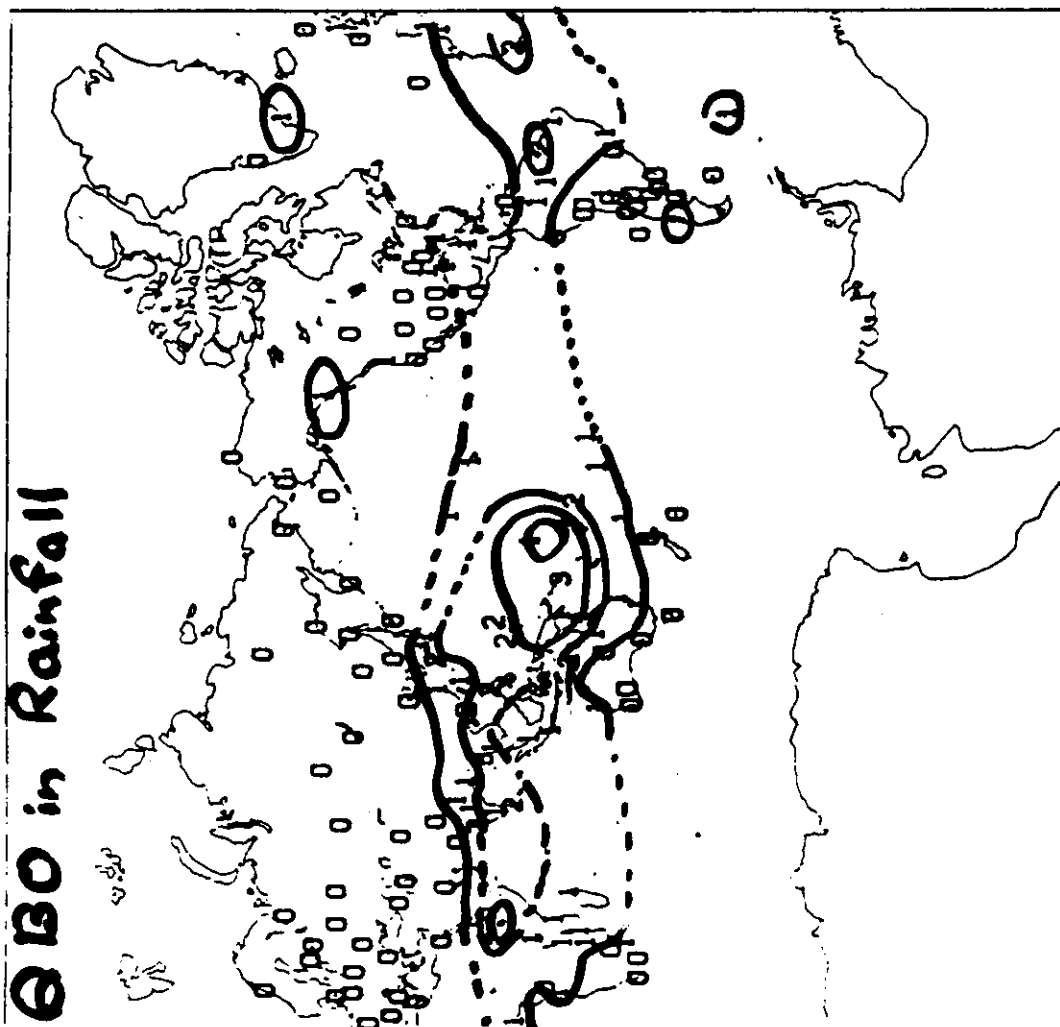


图 1

降水量のQBOの

分布。

0 : < 10

1 : 10 - 20

2 : 20 - 30

3 : 30 - 40

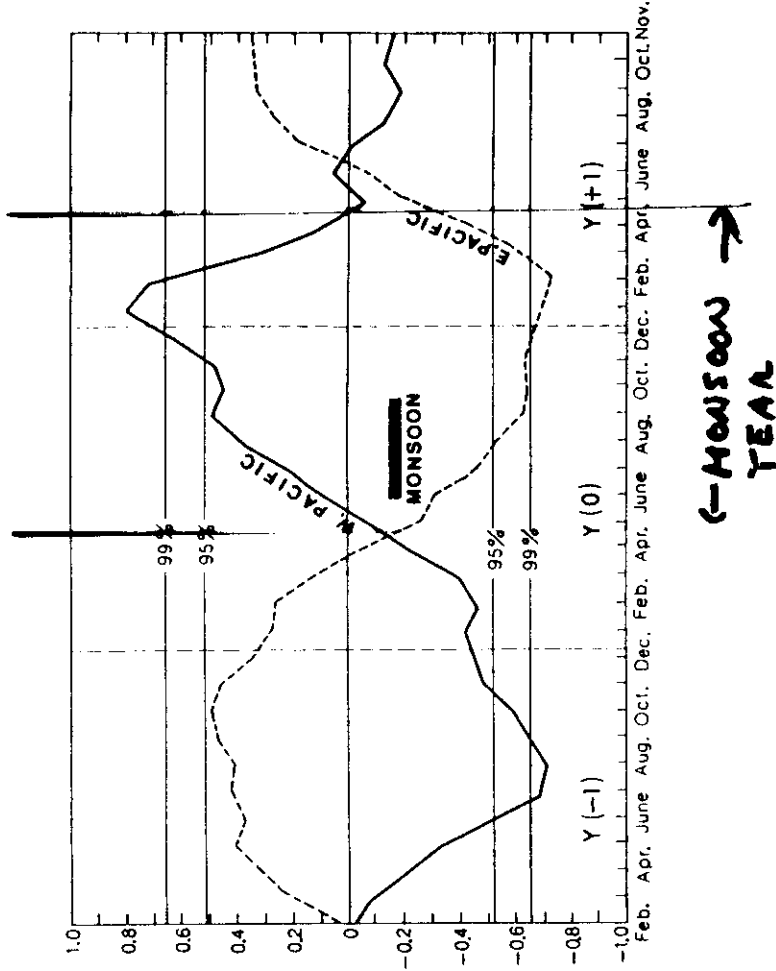
4 : > 40
(単位 : mm/month)

COR.

INDIAN MONSOON RAINFALL VS. SST PACIFIC (0-8N)

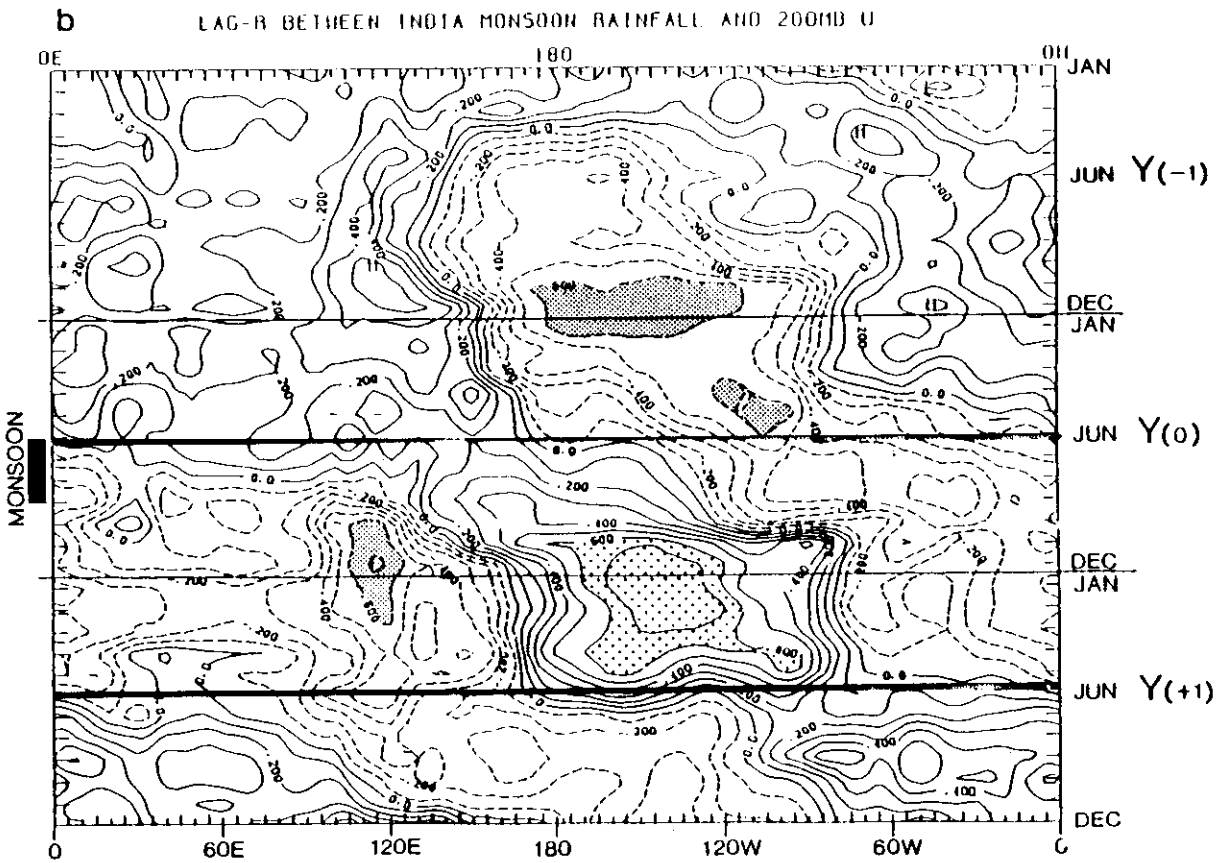
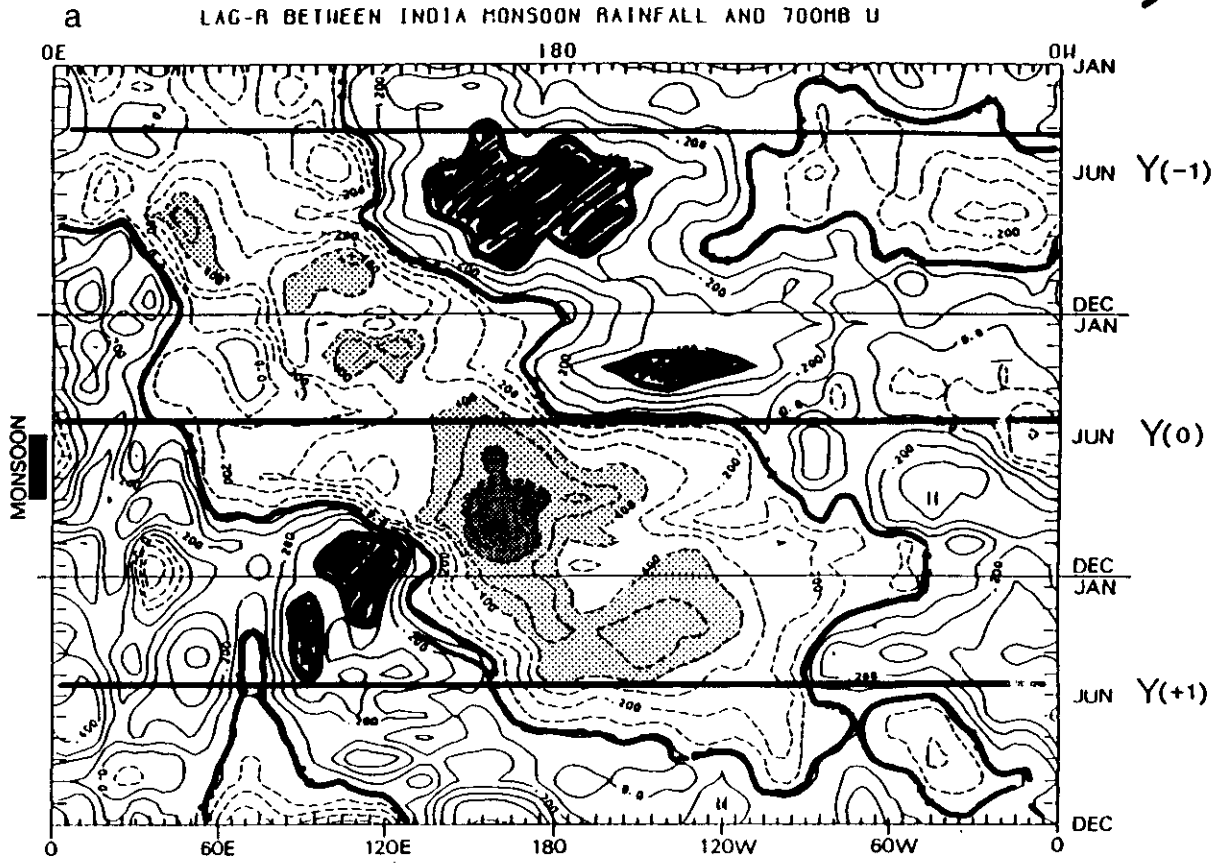
W. (130-150 E)

E (190W-150W)



Yamanari (1990)

IMR vs U700MB (EQ)



アジアモンスーンと大気・海洋結合系 (MAOS)

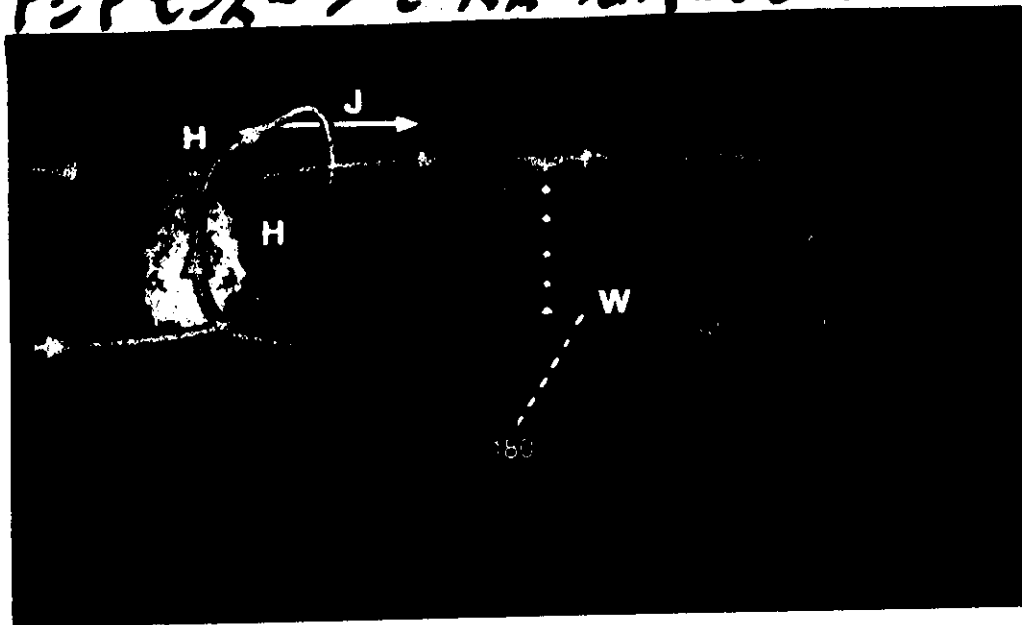


Figure 8b. Schematic illustration (not to scale) of the Walker circulation in the Pacific Basin and its interaction to reinforce (under non-El Niño conditions) the east Asian branch of the Hadley cell. The red area denotes the normally warm SST's in the region of the "maritime continent," which are associated with intense convective rain, as indicated by the cloud. The dashed line just east of the date line depicts the eastward shift of the axis of the upward branch of the Walker cell during an ENSO situation.

Monsoon / Atmosphere-Ocean System (MAOS)

the atmosphere is concentrated into a very narrow latitudinal band is shown in Figures 5 and 10. Figure 10 shows a pre-satellite map of oceanic precipitation (Malkus, 1962) constructed by extrapolating from land and island stations, with the results adjusted so that global water and heat energy budgets are balanced. The lack of precipitation measurements to substantially improve Figure 10, which may have significant errors, has been a major obstacle to the development of Earth system science during the past quarter century. Figure 10 again brings home the latitudinal concentration of the precipitation's heat release and shows that it is the major supply providing the source for the huge poleward export of heat and potential energy; precipitation heating is also the major term which acts toward balancing outgoing radiative heat losses at all latitudes.

In studying the heat budget of the Equatorial Trough Zone and investigating the mechanisms and interacting scales of motion which maintain it, Riehl and Malkus (1958) found the necessity to postulate their "hot tower" hypothesis, which in the past three decades has gained many applications and gradual acceptance in tropical meteorology. They recently repeated the same analyses with vastly more extensive and improved data sources and arrived at essentially the same

results (Riehl and Simpson, 1979). A result relevant to TRMM is summarized in Table 4.

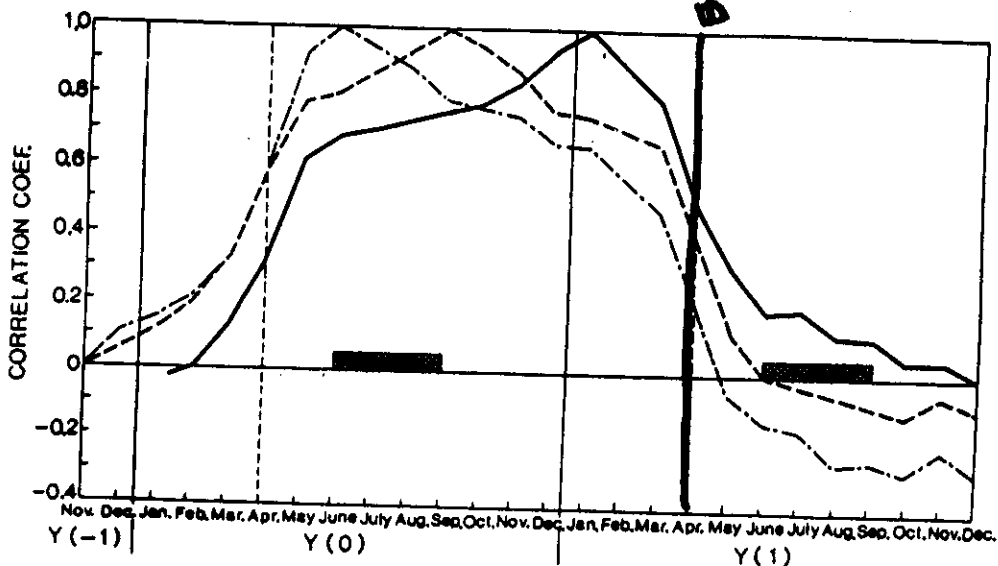
One of the most important findings concerning mechanisms in the atmosphere's Equatorial Trough Zone was that the vertical transports must be effected by large buoyant cumulonimbus cores or "hot towers," which have undergone little or no dilution from the mixing in, or entrainment, of the drier outside air. In conducting their budget study, Riehl and Simpson (1979, *loc. cit.*) were able to estimate the vertical energy flux from the undilute hot towers, and using typical cloud measurements, were able to specify how many towers are needed at one time. This figure comes out to be about 1,600-2,400 cloud towers. The interacting scales involved and the extreme concentration of the "firebox" (or heat release) is brought home by the decadal hierarchy of numbers in Table 4. Clearly, since there are so few cloud cylinders in the atmosphere firebox, and cloud growth is highly dependent on their forcing and their environment, one might expect large circulation variabilities related to variation in the high towers and their latent heat release.

Only now, with the prospect of the TRMM satellite, has it become realistic to expect to begin documenting variabilities in these intense convective cores, their top heights, together

⁴The heat is initially released by the condensation of gaseous water vapor into very small liquid cloud droplets, about 5 to 10 μm in diameter. These droplets must grow by coalescence or other processes to 100 to 300 μm (0.1 to 0.3 mm) before they have sufficient terminal velocities to fall as rain. The rain must reach the Earth or ocean surface to add a net amount of latent heat to the air, for if the small drops remain airborne and evaporate, the condensation heating is reabsorbed. Hence, the shorter expression "precipitation heating" is commonly used.

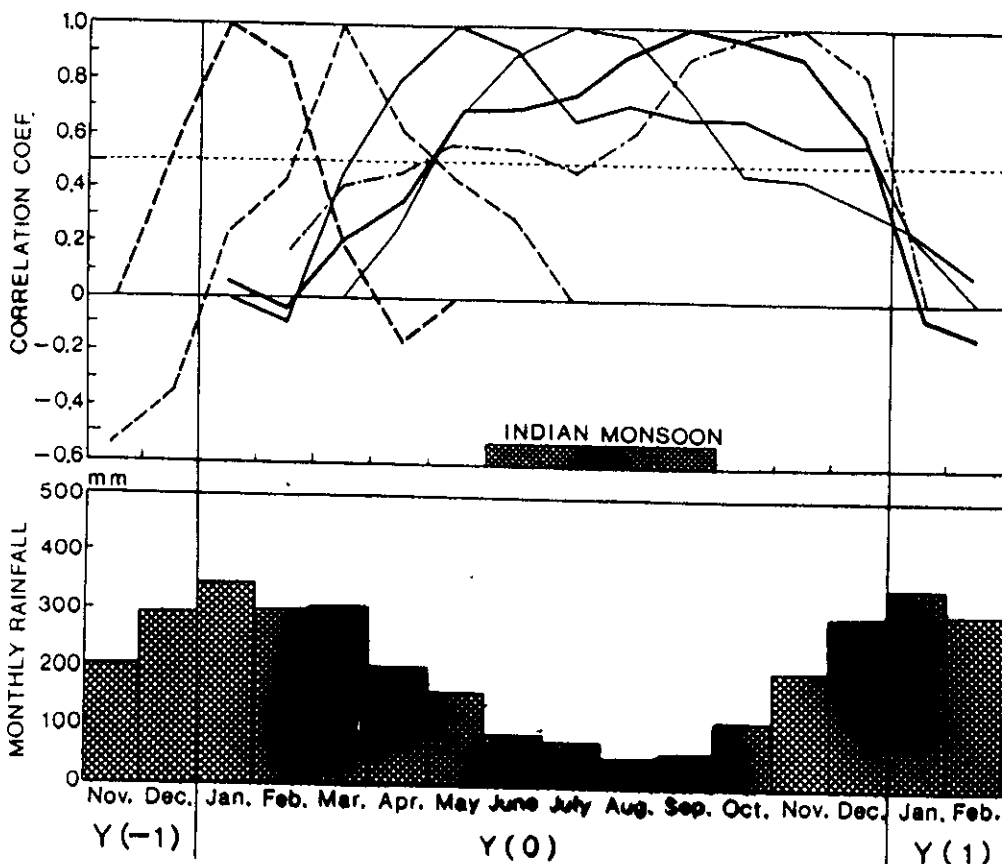
Indian monsoon rainfall vs. SOI.

Predictability Barrier

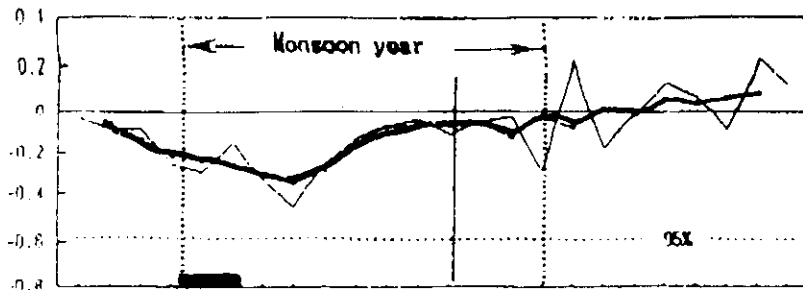


(Yasunari, 1991)

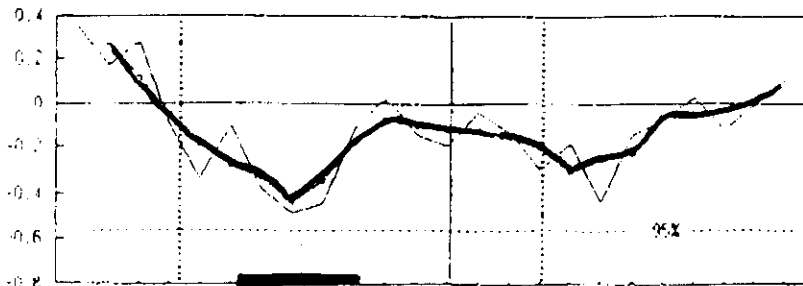
Indonesian rainfall (1970-1971)



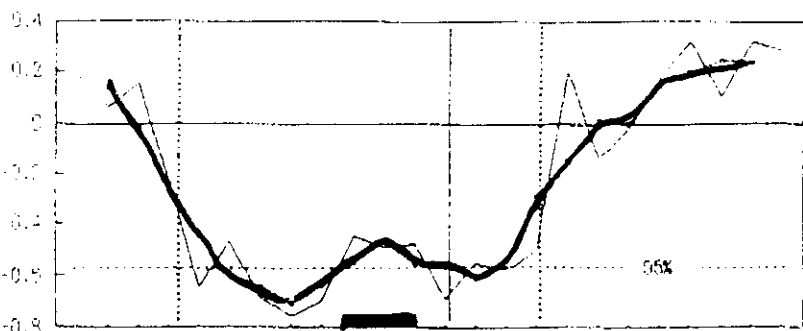
(Yasunari and Sumiati, 1972)



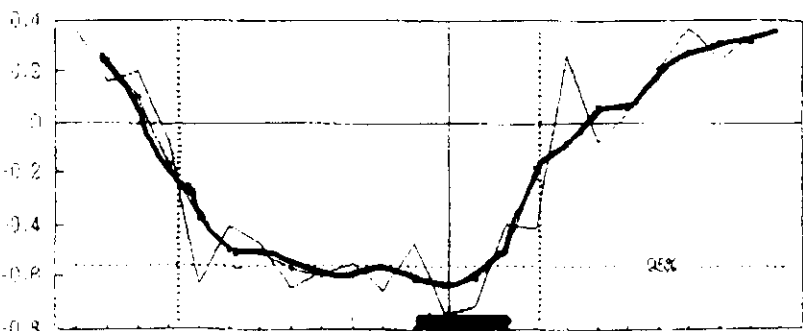
MALAYSIA
SPRING
RAINFALL



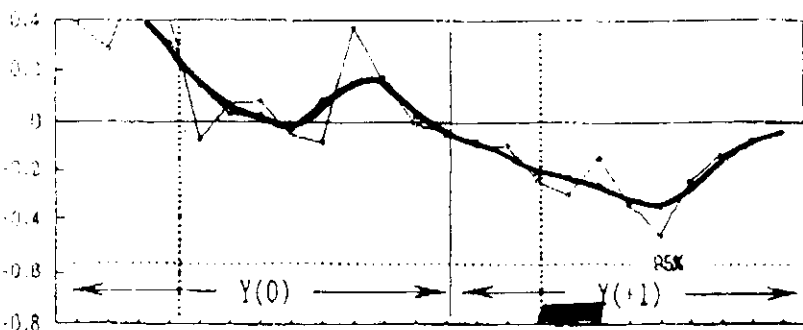
SE Asia
Summer
Monsoon
RAINFALL



MALAYSIA
AUTUMN
RAINFALL



AUSTRALIAN
SUMMER
Monsoon
Rainfall

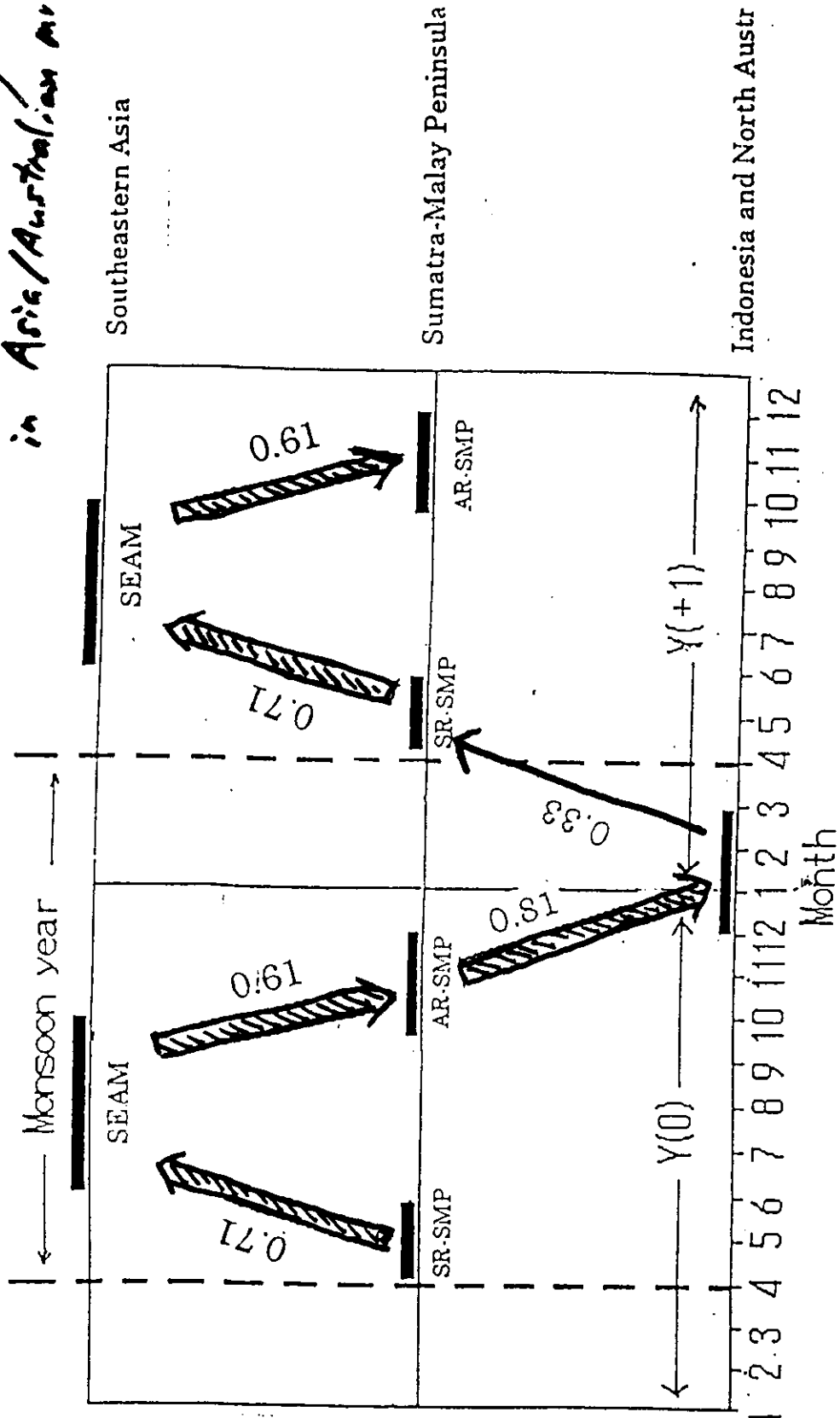


MALAYSIA
-SPRING
RAINFALL

1 2 3 4 5 6 7 8 9 10 11 12 1 2 3 4 5 6 7 8 9 10 11 12
MONTH
Y(0) Y(+1)

図B. モンスーンとSOIの相関係数の季節変化 (Li and Yasunari, 1996)

Fig. 2 (LAA) correlation diagram between convection anomalies in Asia/Australian m.



東南アジア
SE. Asia

EQ. 赤道

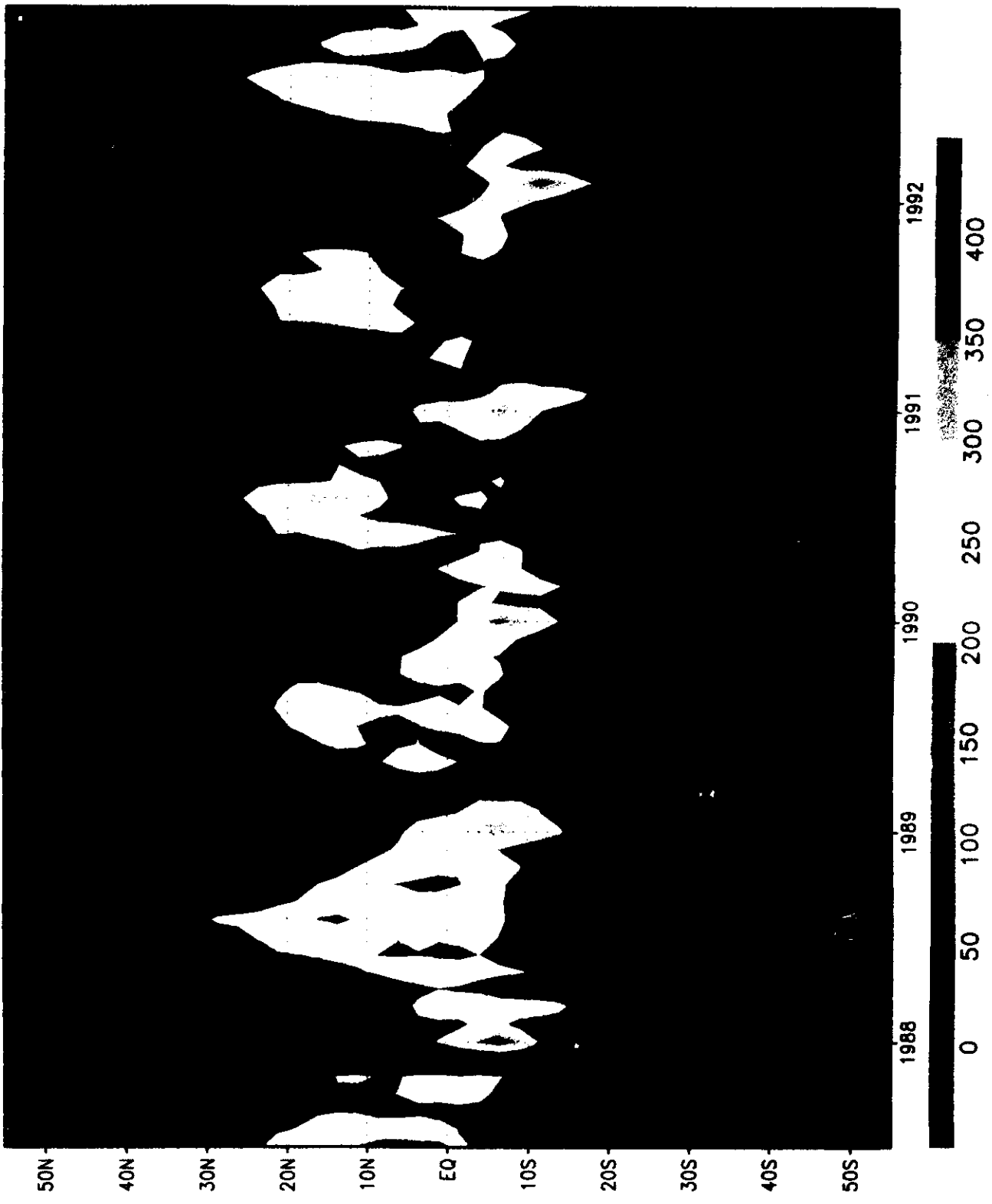
オーストラリア
北西部
N. Australia

(Li and Yasunari, 1996)

Asia/
Mon

GPCP precipitation mm/mo (zonal avg 60E-150E)

by C
of
A.G



o "monsoon year" with
predictability barrier in b. spring.

Then.

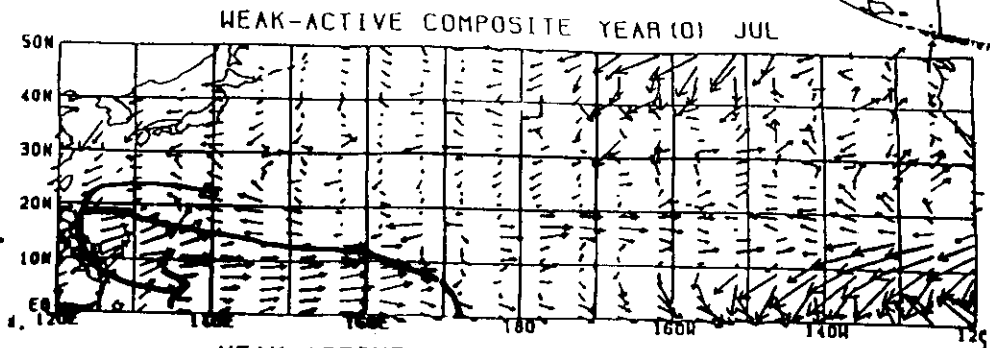
→ How is ^{signals} interannual variability
conveyed from winter to summer?

Signals in the b. spring.

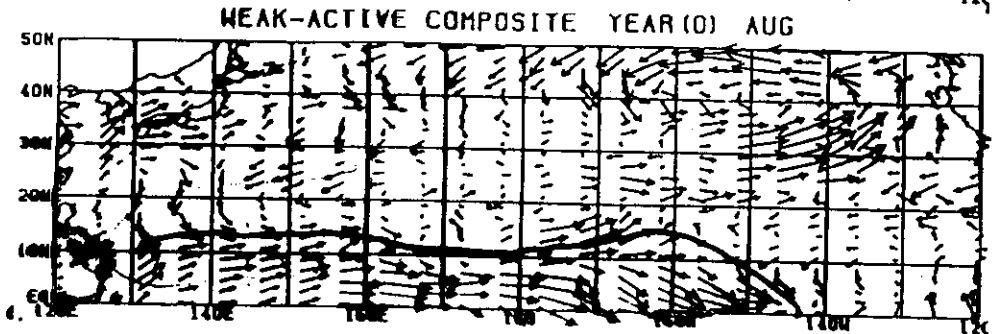
- Eurasian snow cover
- Wind field in sub-tropical
W. Pacific
- SST in South China Sea

Indic
WEAK M.
|
ACTIVE M.

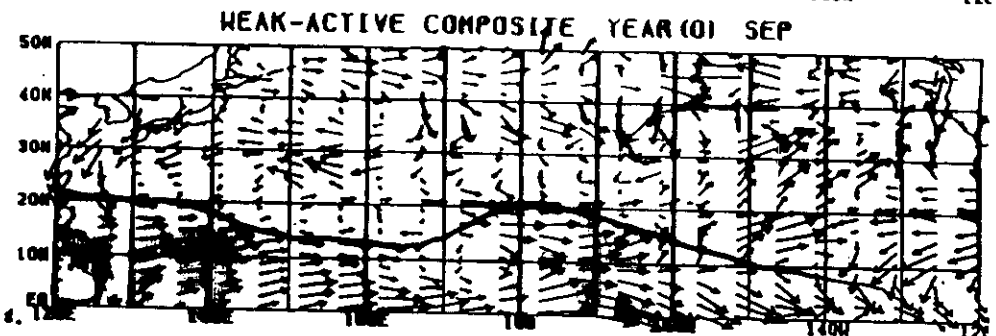
INDIA



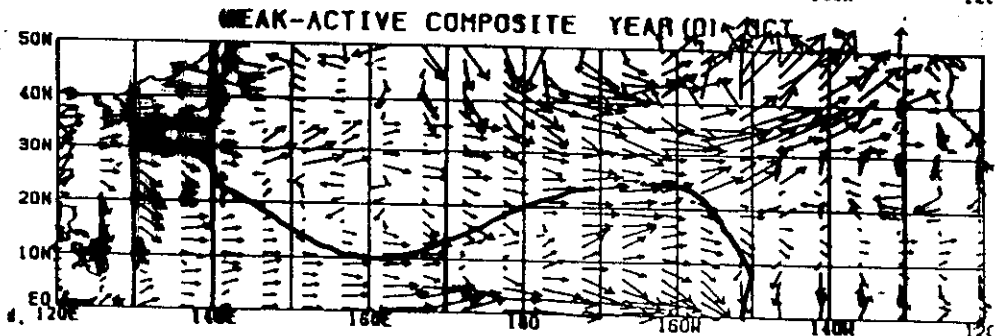
JUL



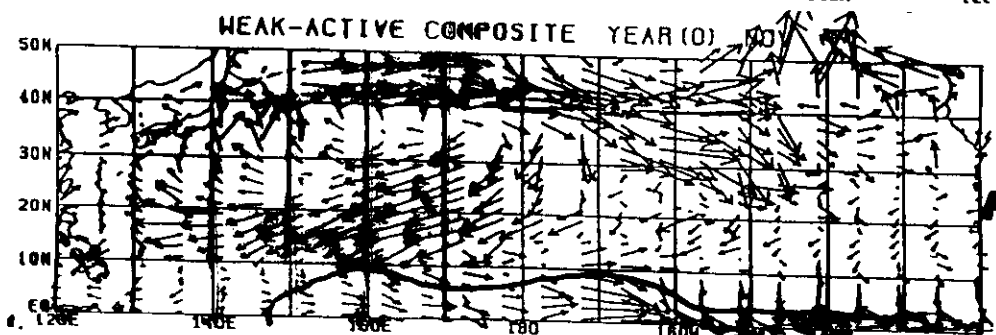
AUG



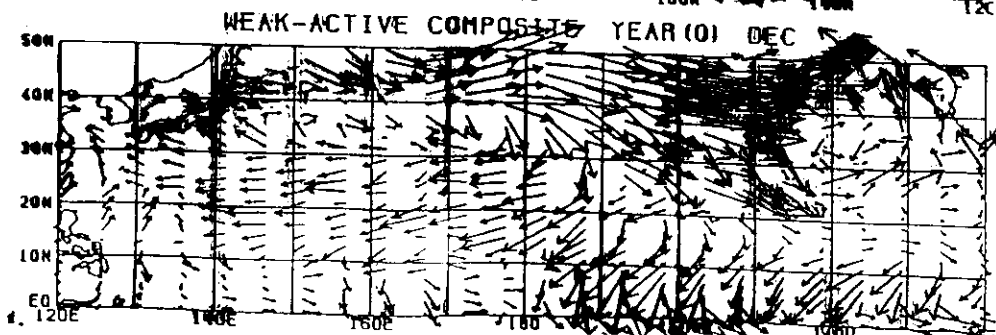
SEP



OCT



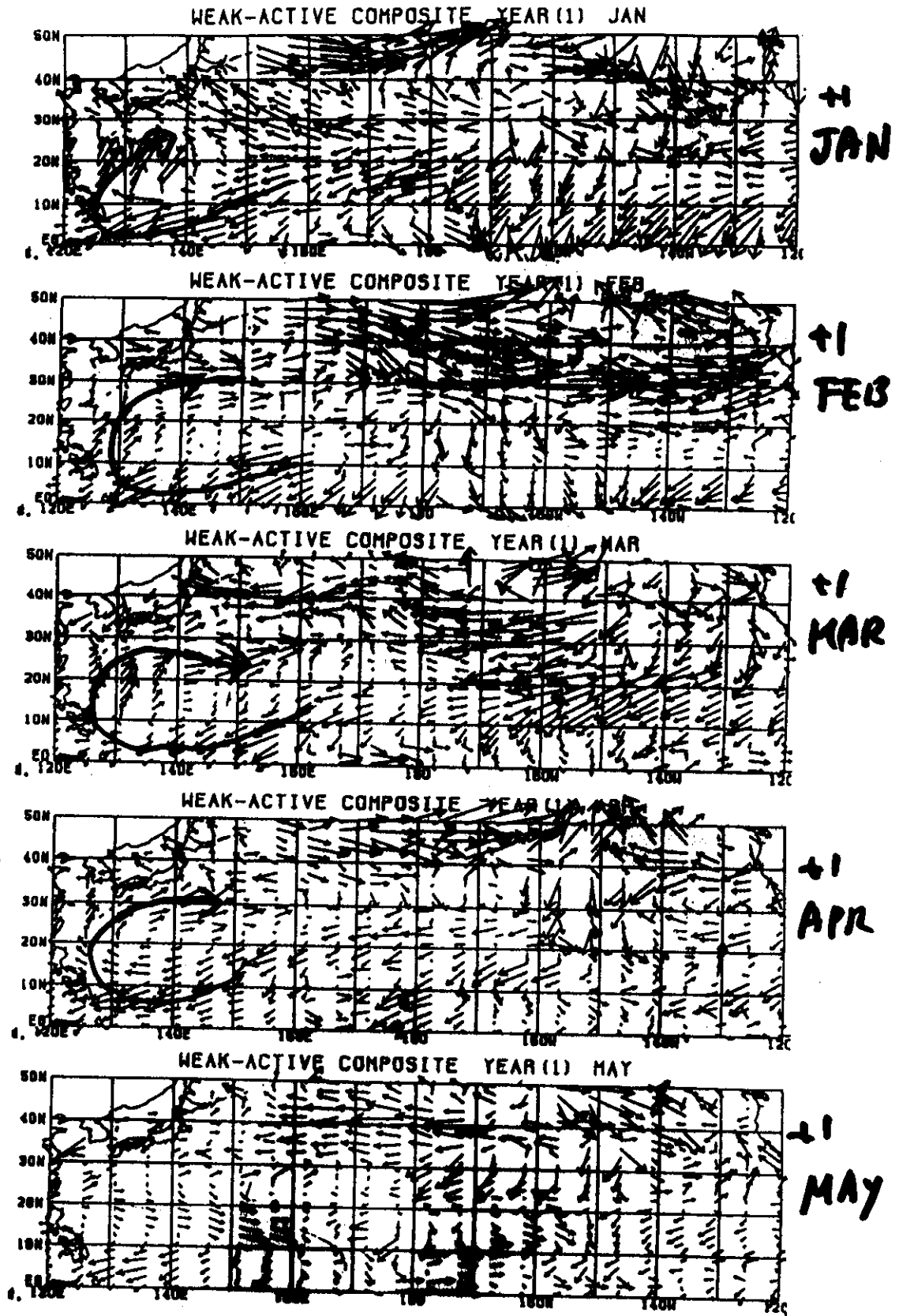
NOV



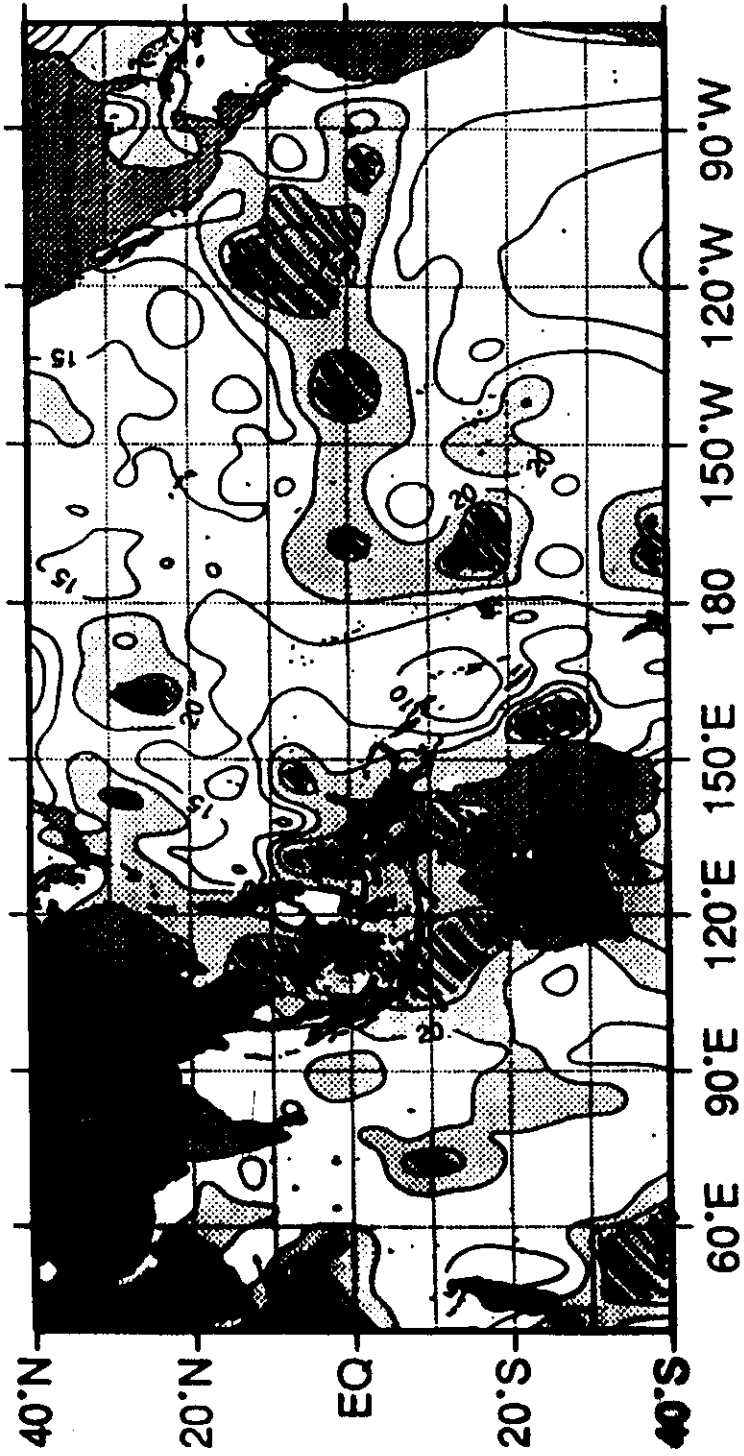
DEC

8

IMR
WEAK
/
ACTIVE

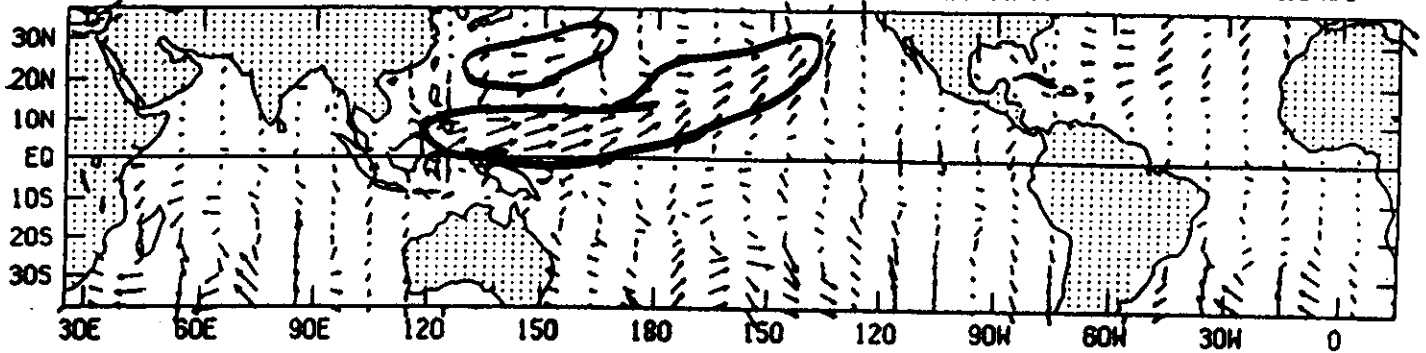


Ratio of σ_B variance to σ_{SST} total variances

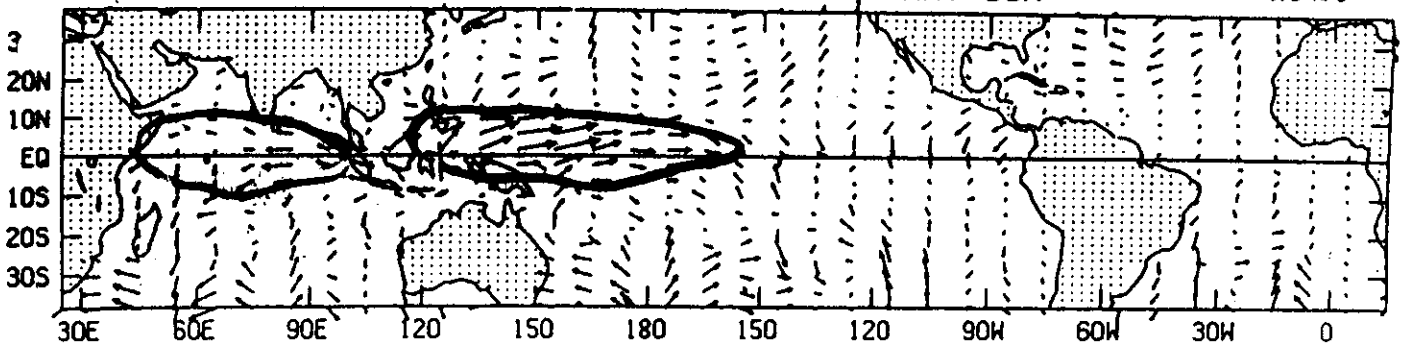


(Tomita and Yasunari, 1995)

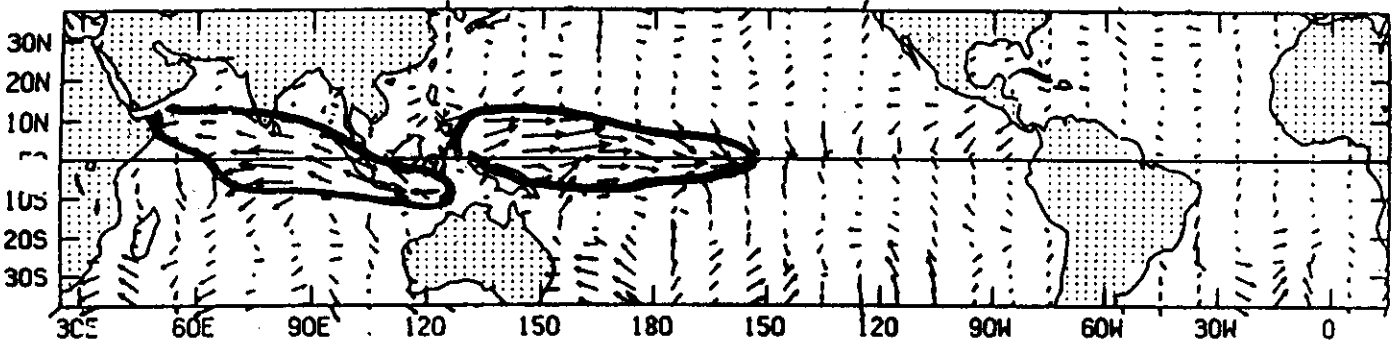
90 E NEGATIVE BIENN. COMPO. WIND FOR MAR-APR



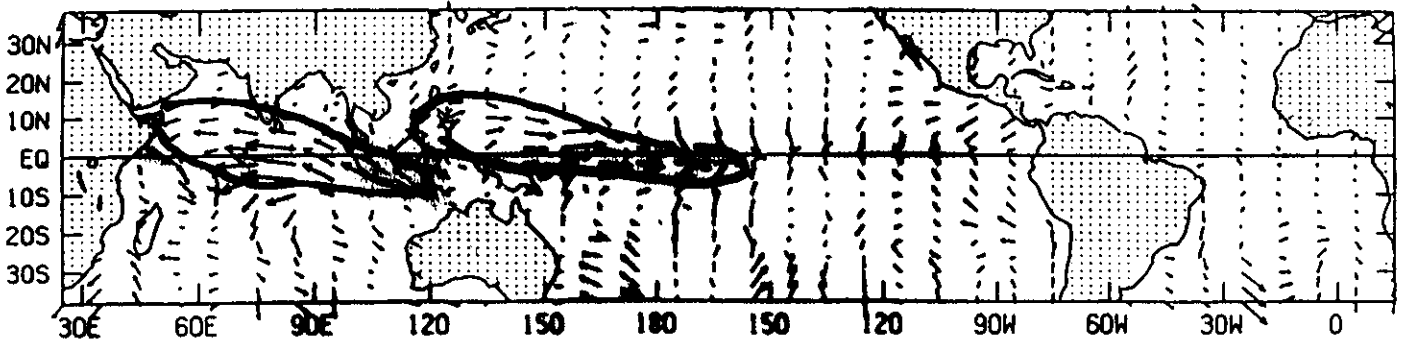
90 E NEGATIVE BIENN. COMPO. WIND FOR MAY-JUN



90 E NEGATIVE BIENN. COMPO. WIND FOR JUL-AUG



90 E NEGATIVE BIENN. COMPO. WIND FOR SEP-OCT



Rasmusson et al. (1989)

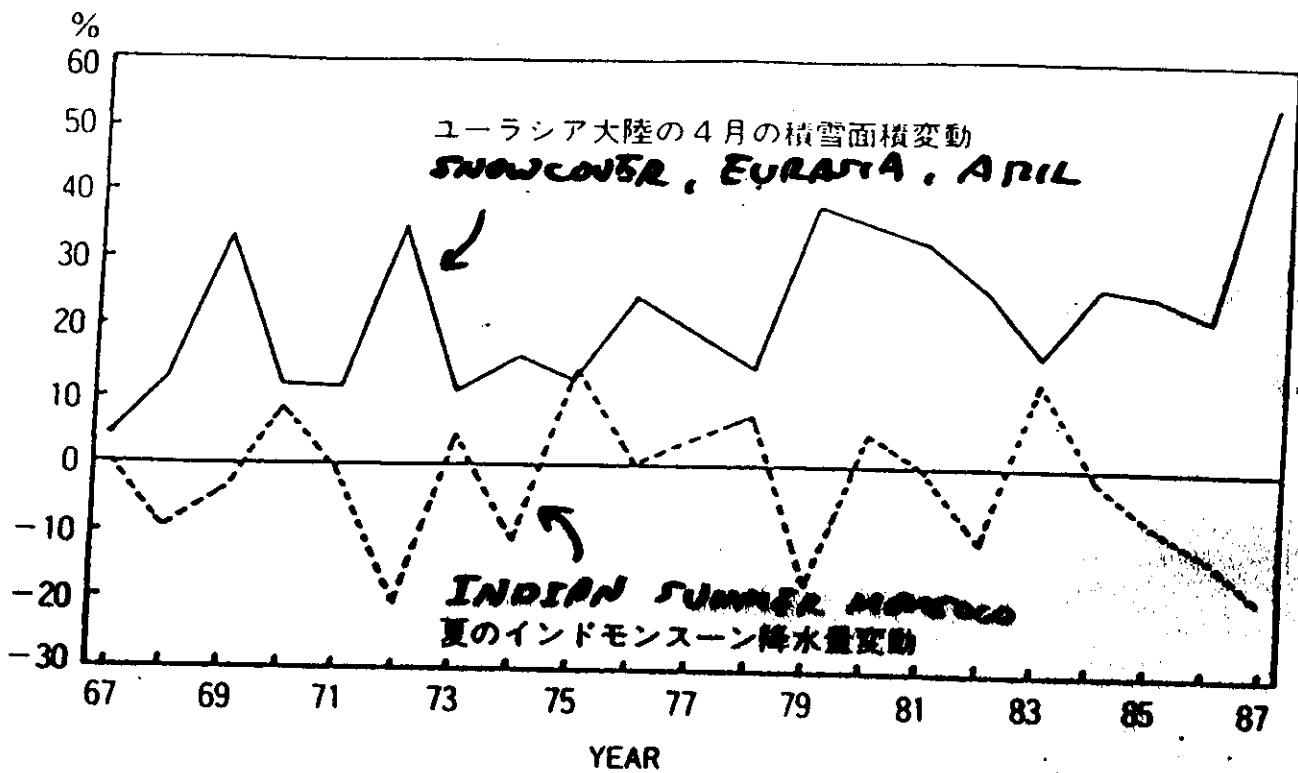


図3 (Morinaga and Yasunari, 1986)

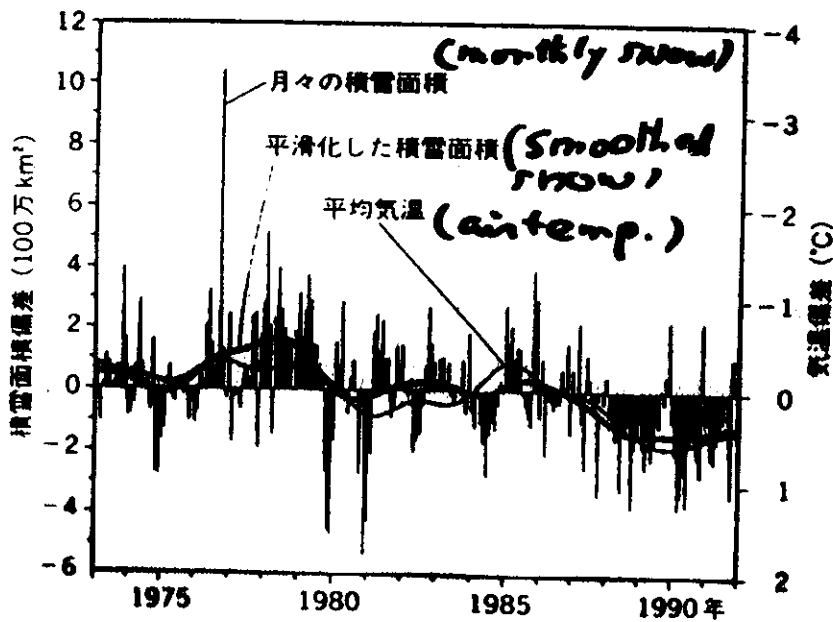


図4 北半球の積雪面積と平均気温の変動。それぞれ平均値からの偏差で表わしている。

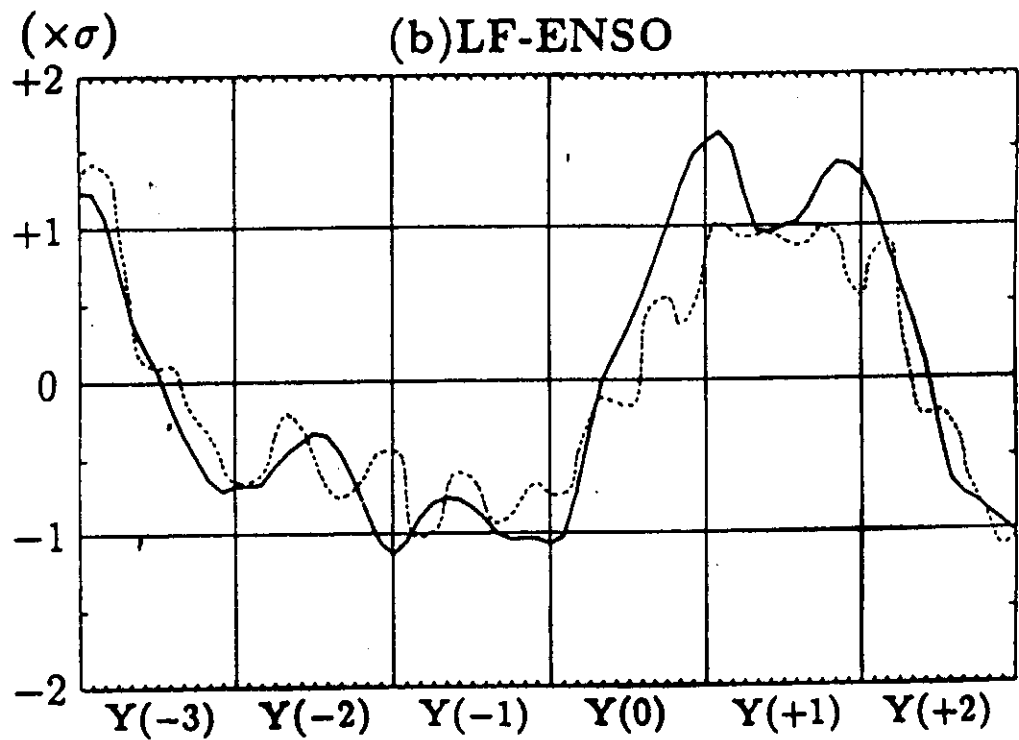
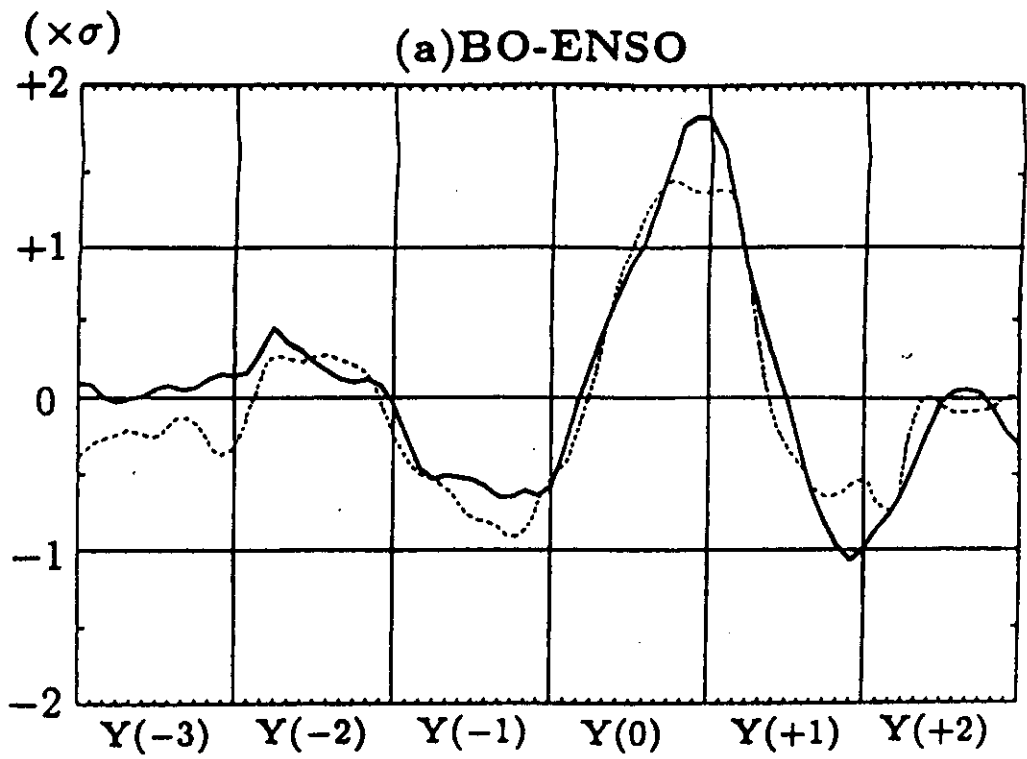
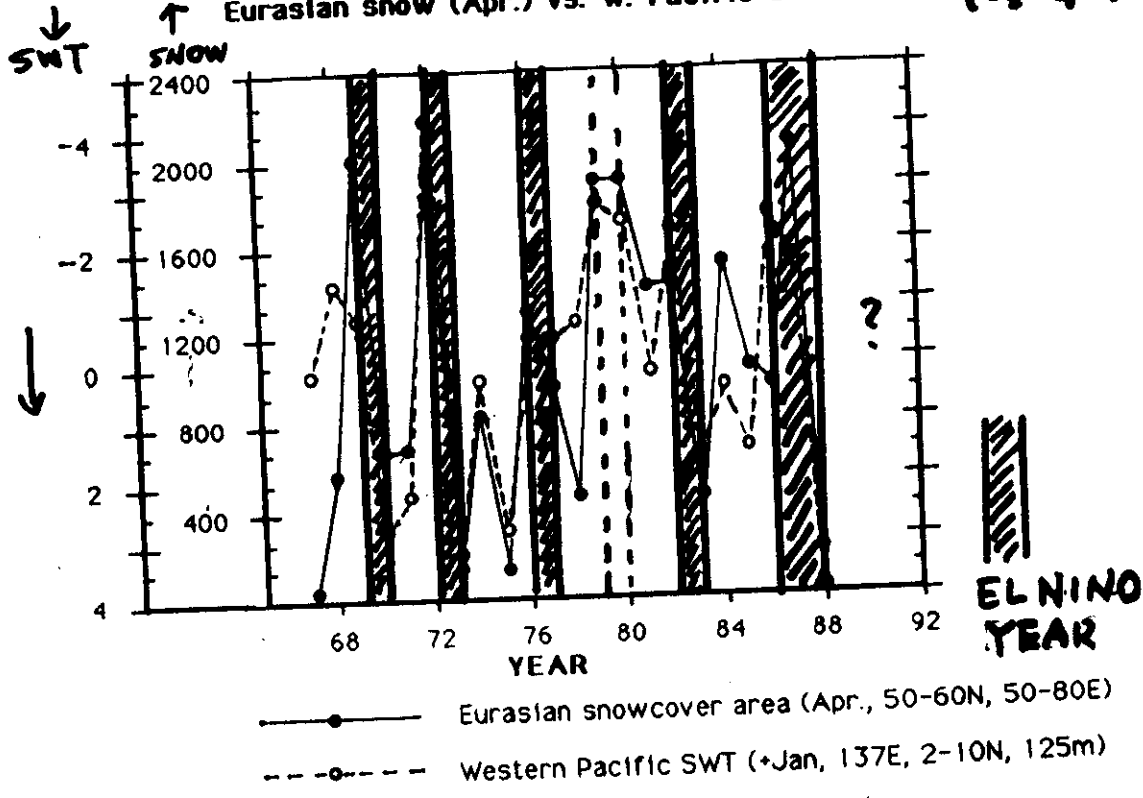


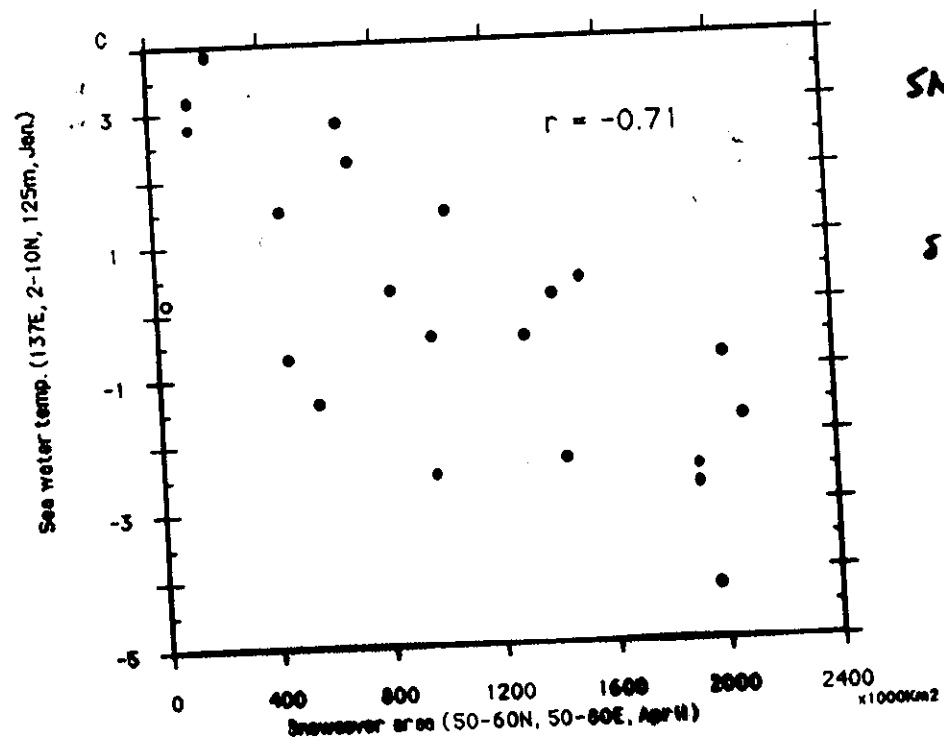
Fig. 3. The composite diagrams of (a) a BO-ENSO and (b) an LF-ENSO using the time series of Fig. 2. Solid (dashed) line indicates the mean SST ($-1 \times$ SOI).

ユーラシアの雪(4A) と 西太平洋浅層水温 (7年1A)
 ↑ Eurasian snow (Apr.) vs. W. Pacific SWT(+Jan) (7年1A)



(Yasunari, 1990b)

Eurasian Snow vs. W. Pacific SWT



CORRELATIONS.

SNOW vs. SWT
 -0.71

SWT vs. IMR
 +0.69

IMR vs. SNOW
 -0.54

SST (DEC-FEB) in South China Sea
and succeeding Indian Monsoon Rainfall

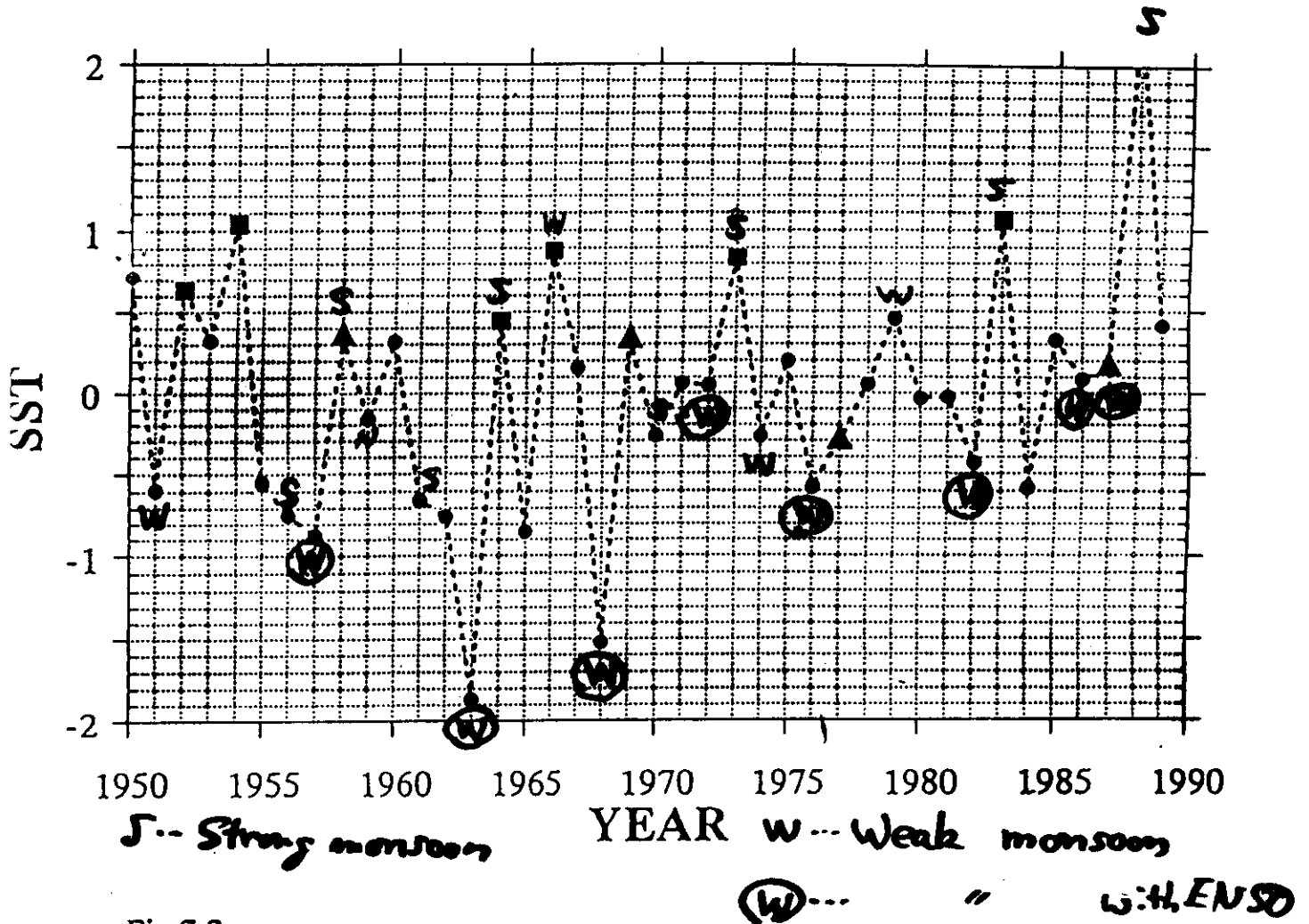


Fig.7.2

Time series of the normalized SST anomalies in the northern winter in South China Sea and the ocean region south of Japan. The square indicates the winter of BO-ENSO from $Y(0)$ to $Y(+1)$ of Fig.5.3 and the triangle indicates that of LF-ENSO.

(Tomita and Yasunari, 1995)

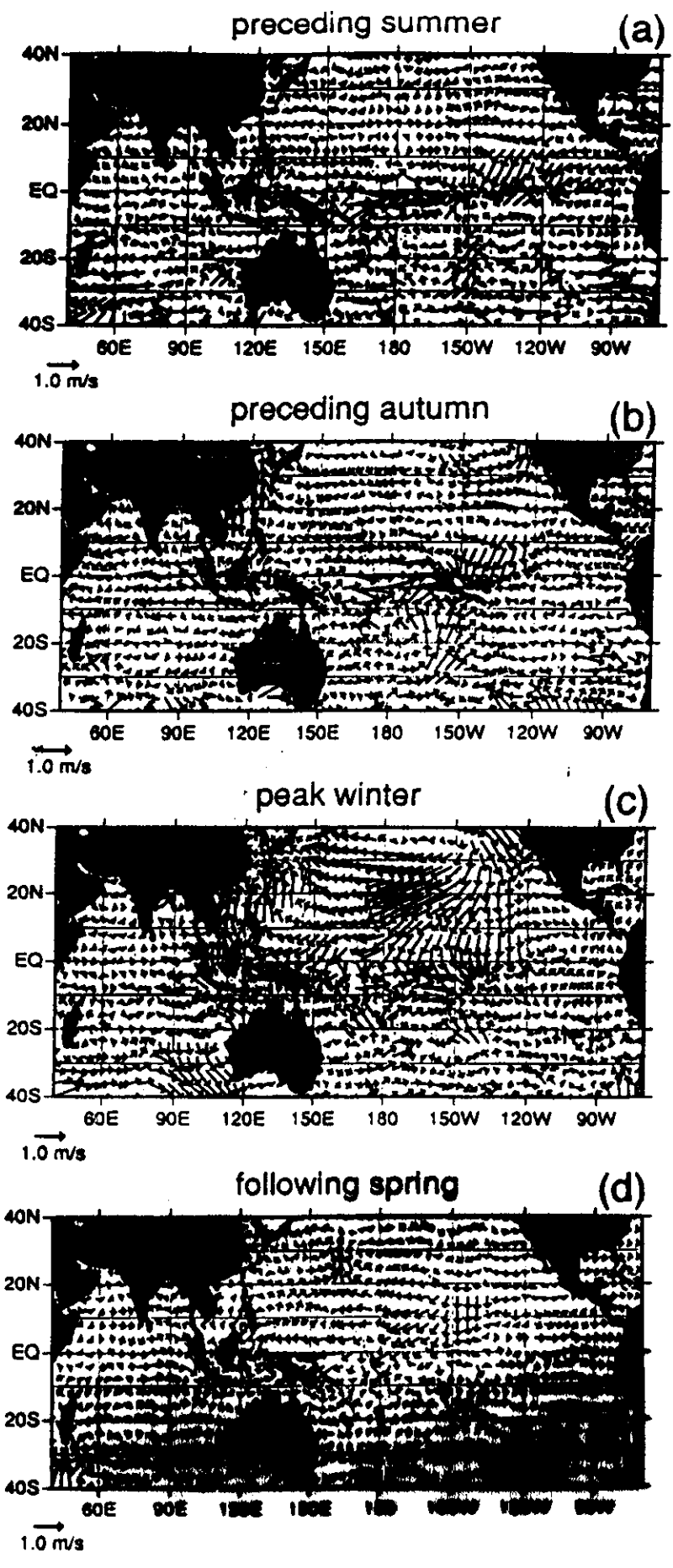


Fig. 7.

STRONG WING



STRONG

WING

STRONG

WING

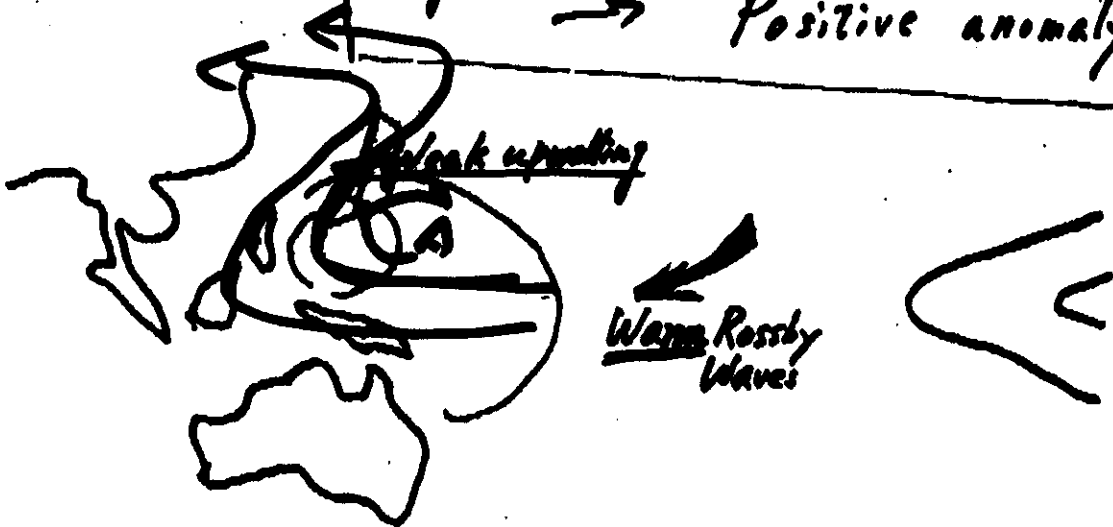
Forced normal mode?

Warm Winter

in East Asia

follows WEAK summer monsoon
precedes active summer monsoon

Negative heat content anomaly
→ Positive anomaly

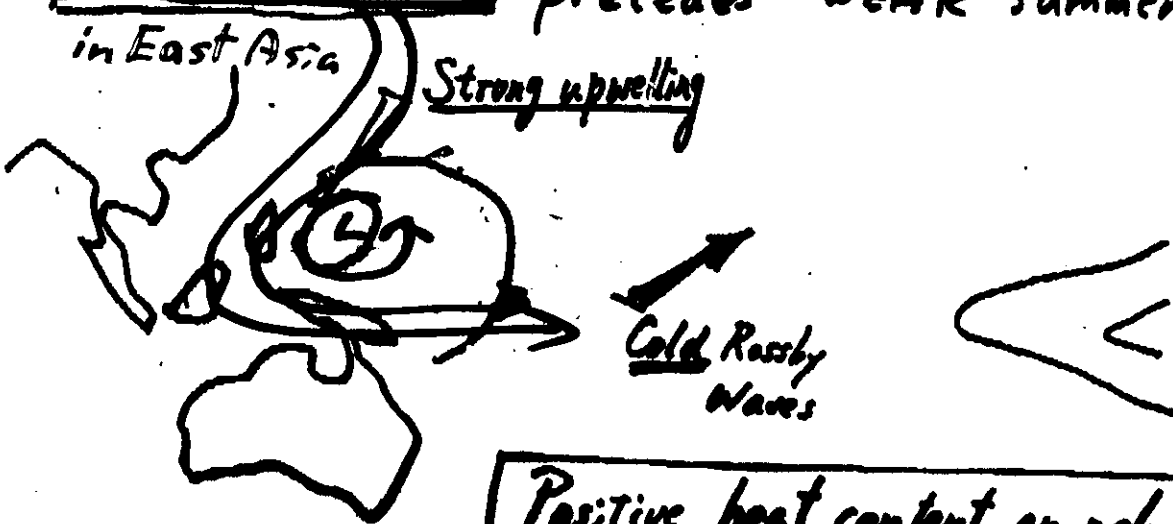


Cold Winter

in East Asia

follows active summer monsoon
precedes WEAK summer monsoon.

Strong upwelling



Positive heat content anomaly
→ Negative anomaly

Masumoto & Yamagata (1990)

Biennial Oscillation of the ENSO/monsoon System

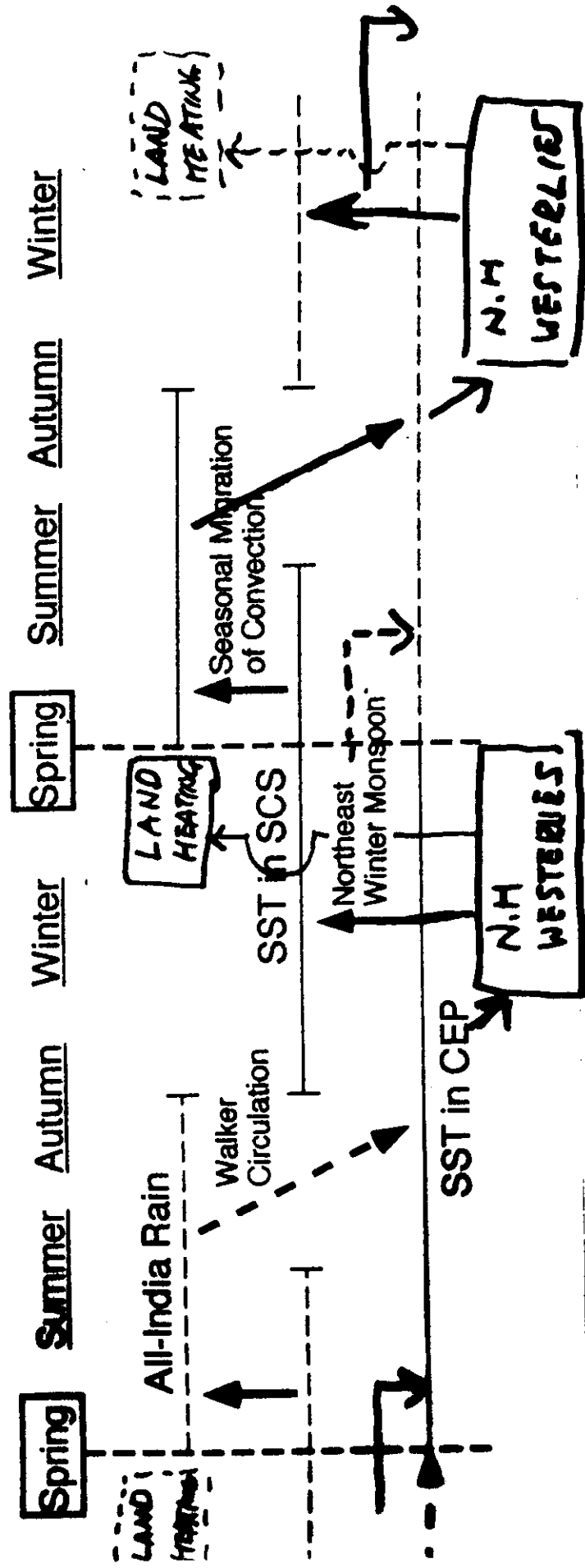


Figure 10 Modified from (Tomita and Yasunari, 1996)

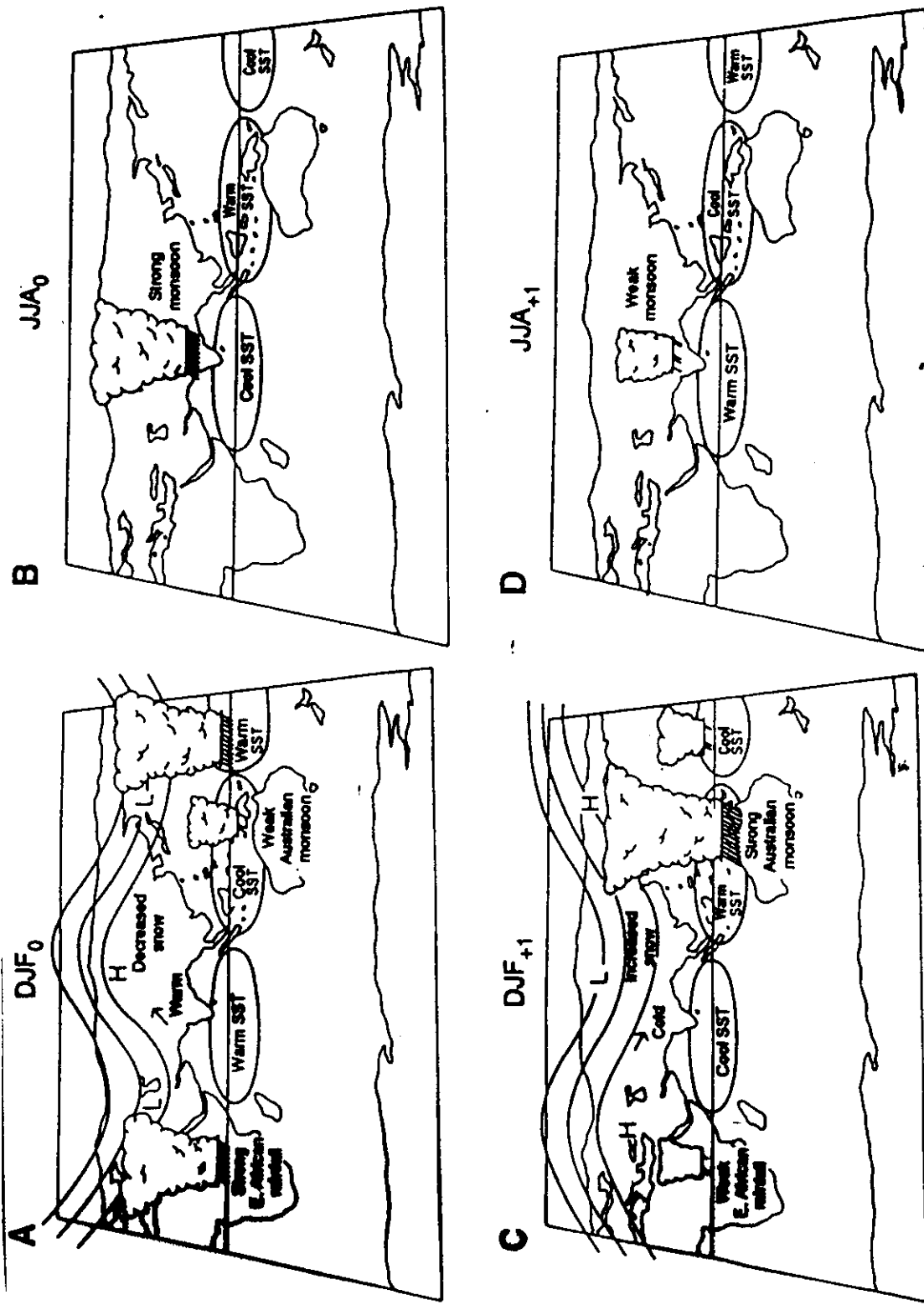


Fig. 8. Schematic biennial evolution from the northern winter before a strong Asian monsoon (A) through the strong monsoon season (B), to the northern winter after the strong monsoon before a weak monsoon (C), to the following weak monsoon (D).

(Meehl, 1994)

Fig. 8



Two basic inherent modes
 in the N.H. westerly flow?
 (in winter)

What controls
ENSO or Non-ENSO
condition
in the Monsoon/ENSO system?

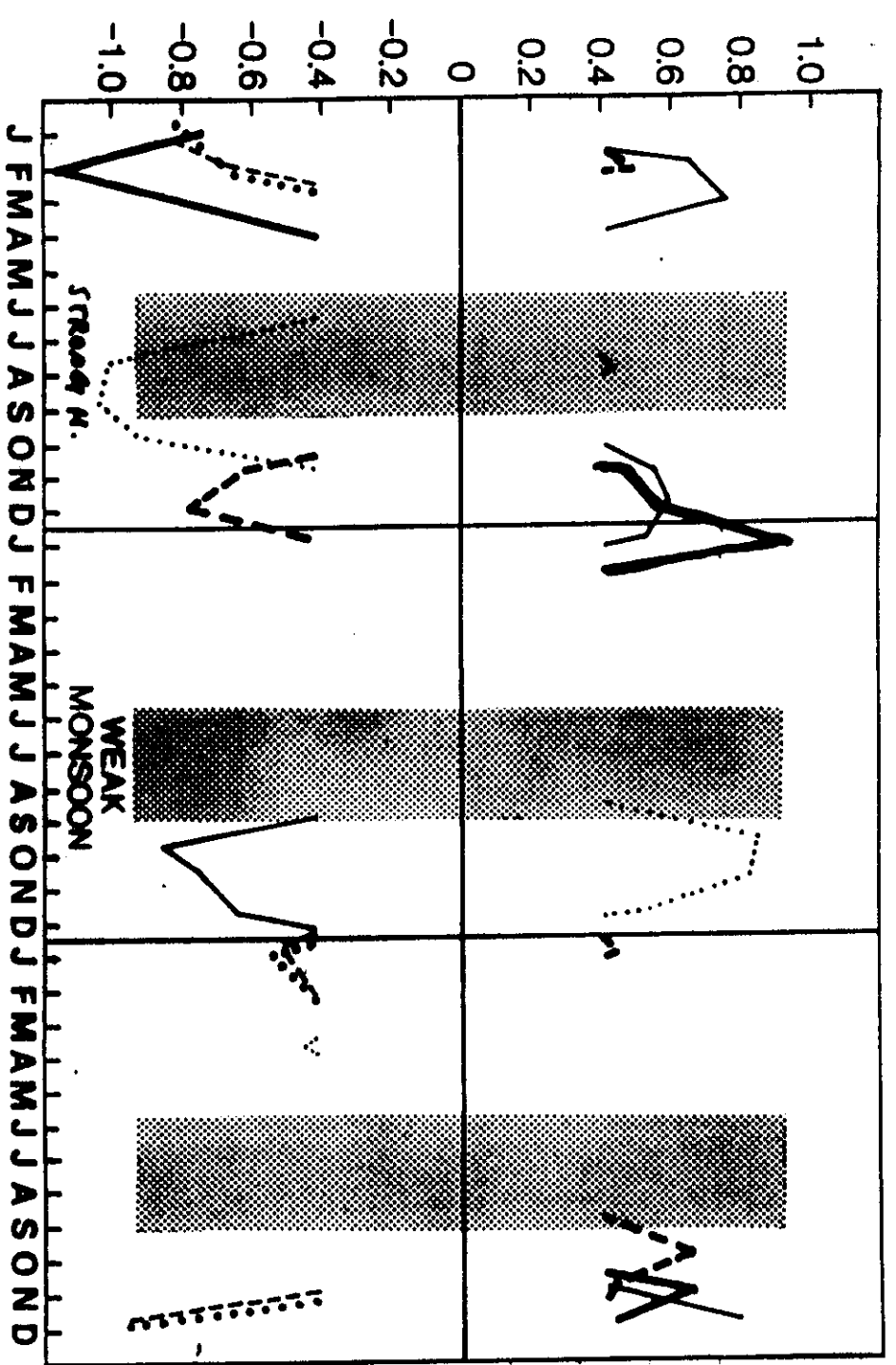
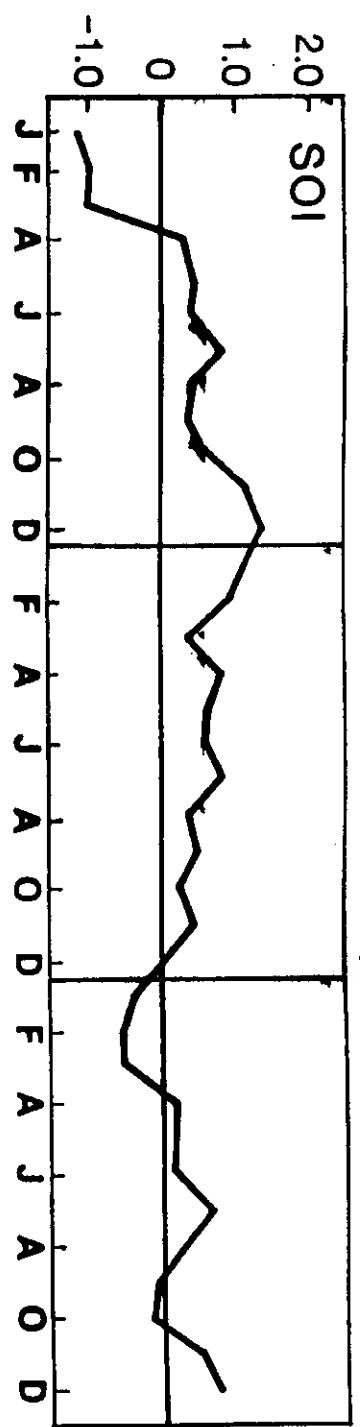
⇒ NAO ?

(which is totally independent
Walker (1932) from SO)

Bennett (1989)

Yasunari and Seki (1992)

WITHOUT ENSO



- NAOI
- PNAI
- PNA
- EU
- ASE
- ANE

Y(-1)

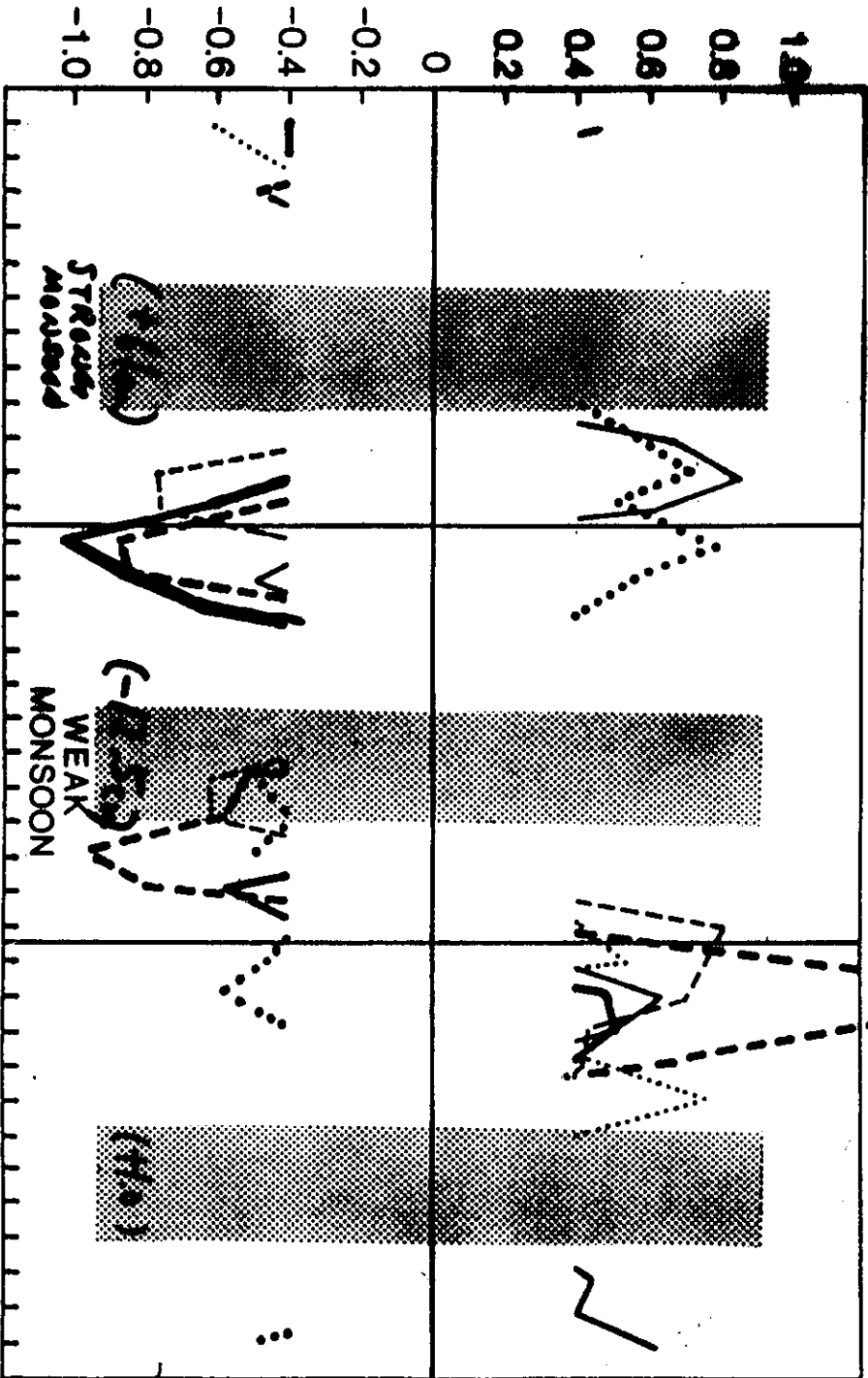
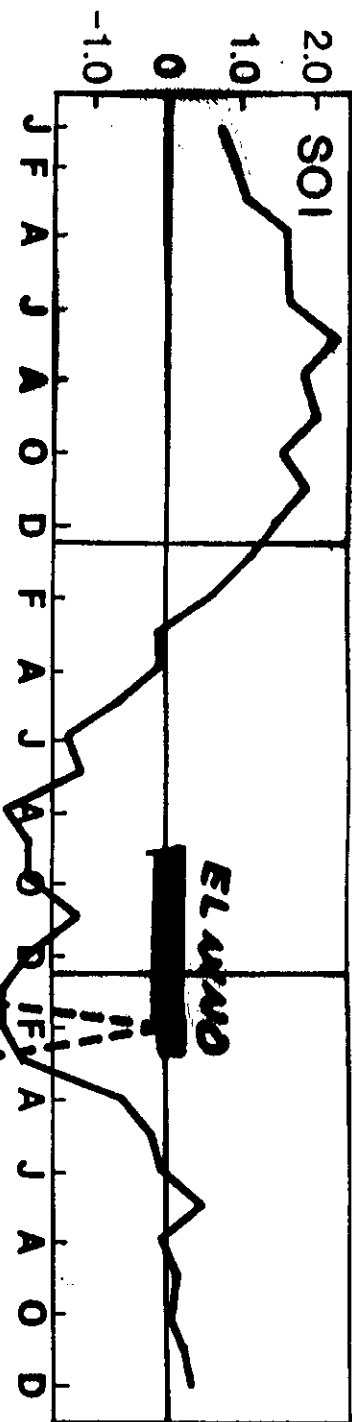
Y(0)

Y(+1)

STRONG N.

WEAK MONSOON

WITH ENSO



- NAO
- PNA I
- PNA II
- EU
- ASE
- ANE

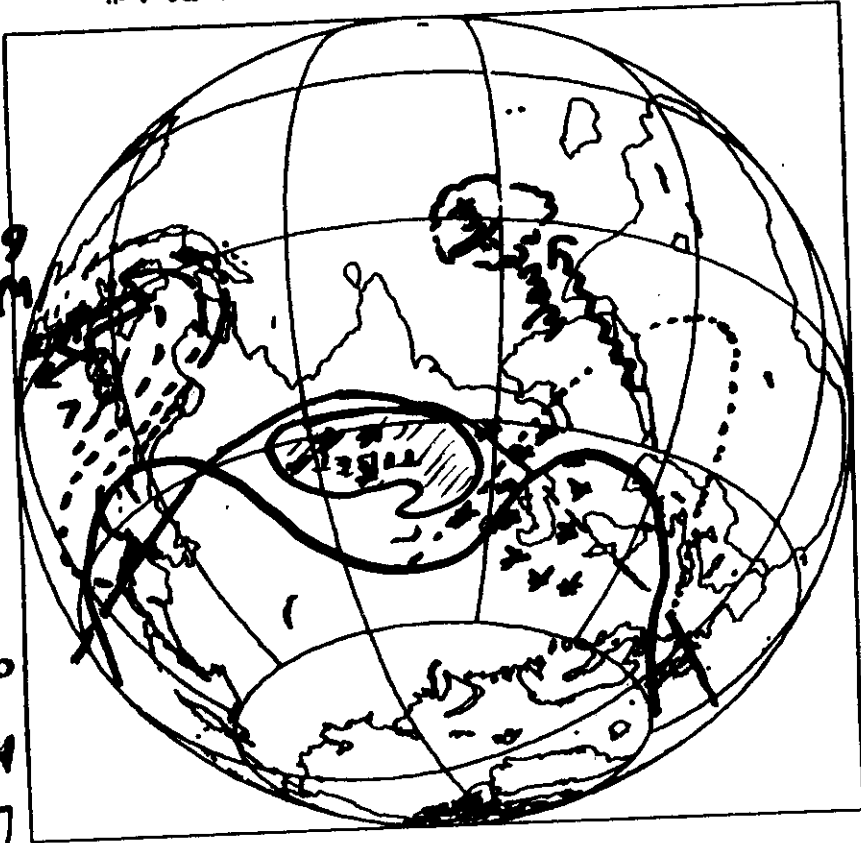
Y(-1)

Y(0)

Y(+1)

J F M A M J J A S O N D J F M A M J J A S O N D J F M A M J J A S O N D

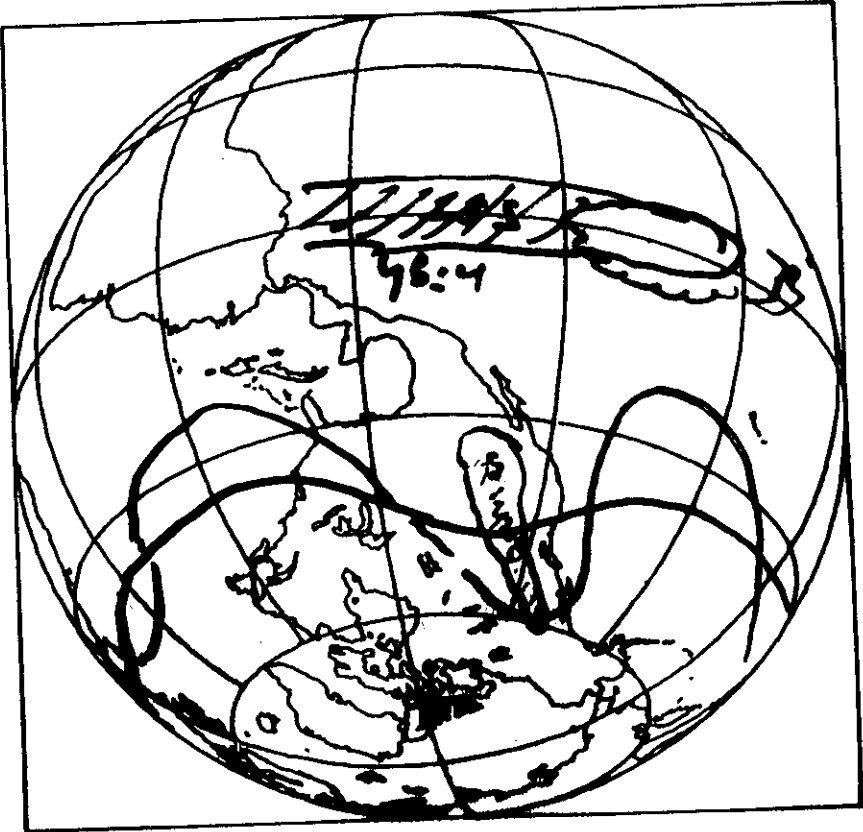
FIGURE 1. THE WIND SYSTEMS OF THE WORLD



Westerly Gird

WINTER
Low Index
High Index
over Eurasia

FIGURE 2. THE WIND SYSTEMS OF THE WORLD



Summary

1. Signals of TBO are prominent in the Asian/Australial monsoon and equatorial Indian/Pacific region

2. Atmosphere-ocean interaction is likely to play an important role in the TBO.

3. TBO in the tropics shows a somewhat different structure from ENSO in the longer time-scale.

4. TBO shows a significant seasonality, by performing the "monsoon year" in the tropics. A distinctive different role is played by the boreal spring and autumn in the interannual variability of the monsoon and the A/O system (MAOS) in the tropics

5. Asian summer monsoon play an essential role in producing an anomalous state in the TBO, whereas the winter monsoon plays an essential role in changing the anomalous state.

6. NAO seems to play a role of modulator for ENSO/non-ENSO state by changing the basic state for the Rossby-wave propagations.

→ 7. E. Asian Winter monsoon & land-surface condition are likely to be coupled each other.

(Seasonal anomalous heating over the Tibetan Plateau is closely linked to SST/convection over SCS & Bay. Bengal.)
(Ueda and Yasunari, 1996) JMSJ. '96. Dec.

